

NATIONAL ADVISORY COMMITTEE FOR AERONAUTICS

TECHNICAL NOTE 2874

ON TRAVELING WAVES IN BEAMS

By Robert W. Leonard and Bernard Budiansky

Langley Aeronautical Laboratory
Langley Field, Va.



Washington

January 1953



CONTENTS

	Page
SUMMARY	1
INTRODUCTION	1
SYMBOLS	2
BASIC EQUATIONS	4
Nonuniform Beams	4
Timoshenko's equations	4
Characteristics and the characteristic form of the equations	6
Propagation of discontinuities	10
Uniform Beams	12
Nondimensional form of the equations	12
Propagation of discontinuities when $c_1 = c_2$	14
Limitations of the Theory	15
SPECIFIC EXAMPLES - FINITE UNIFORM BEAMS WITH $c_1 = c_2$	15
Methods of Solution	15
Cantilever Beam Given a Step Velocity at the Root	16
Simply Supported Beam With an Applied End Moment	17
Step moment	17
Ramp-platform moment	18
CONCLUDING REMARKS	18
APPENDIX A - NUMERICAL SOLUTIONS FOR UNIFORM BEAMS WITH $c_1 = c_2$	20
Matrix Formulation	20
Specific Problems	23
Cantilever beam given a step velocity at the root	23
Simply supported beam with an applied end moment	27
APPENDIX B - MODAL SOLUTIONS FOR UNIFORM BEAMS	31
Equations	31
Specific Problems	33
Cantilever beam given a step velocity at the root	33
Simply supported beam with an applied step end moment	40
Simply supported beam with an applied ramp-platform end moment	47
APPENDIX C - EXACT CLOSED SOLUTIONS FOR UNIFORM BEAMS WITH $c_1 = c_2$	50
Introduction	50
Equations	50
Specific Problems	51

	Page
Infinite cantilever given a step velocity at the root	51
Infinite simply supported beam with an applied step end moment	56
Finite simply supported beam with an applied step end moment	58
Finite simply supported beam with an applied ramp-platform end moment	62
REFERENCES	66
TABLE	68
FIGURES	69

NATIONAL ADVISORY COMMITTEE FOR AERONAUTICS

TECHNICAL NOTE 2874

ON TRAVELING WAVES IN BEAMS

By Robert W. Leonard and Bernard Budiansky

SUMMARY

The basic equations of Timoshenko for the motion of vibrating non-uniform beams, which allow for effects of transverse shear deformation and rotary inertia, are presented in several forms, including one in which the equations are written in the directions of the characteristics. The propagation of discontinuities in moment and shear, as governed by these equations, is discussed.

Numerical traveling-wave solutions are obtained for some elementary problems of finite uniform beams for which the propagation velocities of bending and shear discontinuities are taken to be equal. These solutions are compared with modal solutions of Timoshenko's equations and, in some cases, with exact closed solutions.

INTRODUCTION

The theoretical analysis of transient stresses in aircraft wings and fuselages subjected to impact loadings has generally been performed by means of a mode-superposition method that uses the natural modes of vibration predicted by the elementary engineering theory of beam bending. (See, for example, refs. 1 to 3.) For very sharp impact loadings, however, this approach is known to have certain shortcomings. For sharp impacts of short duration, many modes are often required for a satisfactory degree of convergence (see, for example, ref. 4); in addition, the use of elementary beam theory in the calculation of the higher modes of vibration is inaccurate because of the neglect of, among other factors, the effects of transverse shear deformation and rotary inertia which become increasingly important for higher and higher modes (ref. 5).

A classically recognized alternative to the modal method of calculating transient stresses in elastic bodies is the traveling-wave approach, which seeks to trace directly the propagation of stresses through the body (ref. 3). Although the traveling-wave concept has been successfully used to treat such simple problems as longitudinal and torsional impact of rods, only recently have serious attempts been made to study the transient bending response of beams by this approach. Flügge (ref. 6)

was apparently the first to point out that elementary beam theory could not serve as an adequate basis for the traveling-wave approach since the elementary theory predicts that disturbances propagate with infinite velocity; he showed, however, that a traveling-wave theory could be constructed by modifying the elementary theory, as Timoshenko (ref. 7) did, to include first-order effects of transverse shear deformation and rotary inertia. On the basis of this more accurate theory, Flügge found that discontinuities in moment and shear travel along the beam with finite, and generally distinct, velocities. A similar analysis was carried out independently by Robinson (ref. 8) who, exploiting the hyperbolic nature of Timoshenko's equations, proposed the use of approximate methods of solution and gave some numerical results for a particular example. Pfeiffer (ref. 9) also suggested the possibility of step-by-step solutions by the method of characteristics. In reference 10, Uflyand attempted an analytical solution of Timoshenko's equations for the case of a simply supported beam subjected to a sudden application of load; however, as was shown by Dengler and Goland (ref. 11), Uflyand's work is marred by the fact that he applied boundary conditions that are incorrect for Timoshenko's theory. The only known example of an exact traveling-wave solution based on Timoshenko's theory was presented by Dengler and Goland for the case of an infinitely long beam subjected to a concentrated impulse.

Thus, although the use of Timoshenko's theory as a basis for the transient-stress analysis of beams has been seriously considered, few problems have actually been solved. Additional basic studies of Timoshenko's equations and their solution, particularly for finite-length beams, constitute necessary prerequisites to the development of practical methods of dynamic-stress analysis based on the traveling-wave approach. In the present paper, several specific problems of transient loading of uniform beams of finite length are considered and their solutions by various procedures, all based on the Timoshenko theory, are presented. These procedures are (a) numerical step-by-step integration - the "method of characteristics," (b) mode superposition, and (c) exact closed-form solution. The examples are all for the special case of equal propagation velocities of shear and bending disturbances; only for this case have exact solutions been found in closed form. For the sake of completeness, the presentation of these solutions is preceded by an exposition of the basic equations of Timoshenko's theory, a derivation of the characteristic lines and characteristic forms of these equations, and a discussion of their implications concerning propagation of disturbances.

SYMBOLS

- A cross-sectional area
- E Young's modulus of elasticity

G	shear modulus of elasticity
I	cross-sectional moment of inertia
L	length of finite beam (arbitrary length for infinite beam)
M	internal bending moment (see fig. 1)
\bar{M}	dimensionless internal bending moment, ML/EI_B
$R = \left(\frac{c_2}{c_1}\right)^2 \left(\frac{L}{r_1}\right)^2$	
V	vertical shear force on a cross section (see fig. 1)
\bar{V}	dimensionless vertical shear force, VL^2/EI_B
c_1	propagation velocity of bending discontinuities, $\sqrt{\frac{EI_B}{\rho I_1}}$
c_2	propagation velocity of shear discontinuities, $\sqrt{\frac{A_S G}{\rho A_1}}$
p	operator used in the Laplace transformation
q	intensity of distributed external loading
\bar{q}	dimensionless intensity of external loading, qL^3/EI_B
r	cross-sectional radius of gyration
t	time
v	velocity of deflection, y_t
\bar{v}	dimensionless velocity of deflection, v/c_2
x	coordinate along beam
y	deflection (see fig. 1)
\bar{y}	dimensionless deflection, y/L
δ	denotes a discontinuity in quantity immediately following
$\lambda = \frac{1}{2} \frac{L}{r_1}$	

ξ	dimensionless coordinate along beam, x/L
ρ	density of beam material
τ	dimensionless time, $c_1 t/L$
ψ	rotation of cross section about neutral axis (see fig. 1)
ω	velocity of rotation of cross section, ψ_t
$\bar{\omega}$	dimensionless velocity of rotation, $\omega L/c_1$

Subscripts:

B	contributing to resistance of beam to bending
i	contributing to inertia
S	contributing to resistance of beam to shearing
x, t, ξ, τ	indicate partial derivatives with respect to those quantities

BASIC EQUATIONS

Nonuniform Beams

Timoshenko's equations. - The Timoshenko theory of beam bending (ref. 7) constitutes a modification of elementary beam theory that attempts to account for the effects of transverse shear deformation and rotary inertia; the basic assumption of elementary theory - that plane sections remain plane - is retained. The moment M , shear V , deflection y , and cross-sectional rotation ψ of a nonuniform beam subject to a dynamic lateral loading q are governed, according to this theory, by the following four simultaneous partial-differential equations (see fig. 1):

$$M + EI_B \psi_x = 0 \quad (1a)$$

$$V - A_S G (y_x - \psi) = 0 \quad (1b)$$

$$M_x - V + \rho I_1 \psi_{tt} = 0 \quad (1c)$$

$$V_x - \rho A_1 y_{tt} + q = 0 \quad (1d)$$

The first two equations constitute elastic laws relating the deformations to the internal loading. Equation (1a) expresses the same relationship between moment and cross-sectional rotation as that given by elementary beam theory. Equation (1b) stipulates a linear relationship between the shear V and the shear angle $y_x - \psi$ at the neutral axis; A_g is the so-called "effective" shear-carrying area, different from the total area A_1 since the true shear angle actually varies over the cross section. Equations (1c) and (1d) prescribe rotational and translational equilibrium, respectively, with the term $\rho I_1 \psi_{tt}$ representing the contribution of rotary inertia.

The moment and shear may be eliminated from equations (1) to yield two simultaneous partial-differential equations in y and ψ :

$$\left. \begin{aligned} (EI_B \psi_x)_x + A_g G (y_x - \psi) - \rho I_1 \psi_{tt} &= 0 \\ [A_g G (y_x - \psi)]_x - \rho A_1 y_{tt} + q &= 0 \end{aligned} \right\} \quad (2)$$

This form is convenient for finding the normal modes and frequencies of free vibration ($q = 0$) predicted by Timoshenko's theory and for carrying out modal analyses that make use of these modes. In this theory, a natural mode is described by a pair of functions $[y(x), \psi(x)]$ rather than a single function $y(x)$, as is the case in elementary beam theory.

For a traveling-wave analysis, however, it is advantageous to return to the original system of equations (eqs. (1)) but to put them in a more convenient form by differentiating equations (1a) and (1b) with respect to time. The equations become:

$$\omega_x + \frac{1}{EI_B} M_t = 0 \quad (3a)$$

$$v_x - \frac{1}{A_g G} V_t - \omega = 0 \quad (3b)$$

$$M_x + \rho I_1 \omega_t - V = 0 \quad (3c)$$

$$V_x - \rho A_1 v_t + q = 0 \quad (3d)$$

where the new variables, linear velocity v and angular velocity ω , have been introduced for y_t and ψ_t , respectively.

Equations (3) comprise four first-order linear partial-differential equations in the four variables v , ω , M , and V . Furthermore, equations (3a) and (3c) contain derivatives of only M and ω , whereas equations (3b) and (3d) contain derivatives of only v and V . These facts are exploited in the next section in seeking characteristic lines, and characteristic forms, of these equations.

Characteristics and the characteristic form of the equations.- In equations (3a) and (3c), the variables M and ω are differentiated with respect to both space and time; it would be advantageous to replace them by equivalent equations each involving only total derivatives (or differentials) in a particular direction in the space-time plane. The lines in the space-time plane having these particular directions - the characteristic lines or so-called "characteristics" - and the equivalent equations written in these directions are found as follows (ref. 12).

A linear combination of equations (3a) and (3c),

$$\mu(M_t + EI_B \omega_x) + M_x + \rho I_1 \omega_t - V = 0 \quad (4)$$

is formed, where the function μ is to be determined in such a way that the partial derivatives in equation (4) combine to give total derivatives $\frac{dM}{d\sigma}$ and $\frac{d\omega}{d\sigma}$ in the direction of an as yet unknown characteristic line $[x(\sigma), t(\sigma)]$. In order that the terms involving derivatives of M combine in the form

$$M_x \frac{dx}{d\sigma} + M_t \frac{dt}{d\sigma} = \frac{dM}{d\sigma}$$

the function μ must satisfy the following equation:

$$\mu = \frac{\frac{dt}{d\sigma}}{\frac{dx}{d\sigma}} = \frac{dt}{dx}$$

where $\frac{dt}{dx}$ is the required slope of the characteristic line. Similarly, in order that the terms involving derivatives of ω combine in the form

$$\omega_x \frac{dx}{d\sigma} + \omega_t \frac{dt}{d\sigma} = \frac{d\omega}{d\sigma}$$

the function μ must also satisfy the equation

$$\frac{\rho I_1}{\mu E I_B} = \frac{\frac{dt}{d\sigma}}{\frac{dx}{d\sigma}} = \frac{dt}{dx}$$

Since the characteristic slope must be the same in both cases, μ is defined by

$$\mu^2 = \frac{\rho I_1}{E I_B}$$

Thus, the two values of μ and the corresponding characteristic slopes $\frac{dt}{dx}$ are:

$$\left. \begin{aligned} \mu &= \frac{1}{c_1} \\ \frac{dt}{dx} &= \frac{1}{c_1} \end{aligned} \right\} \quad (5)$$

$$\left. \begin{aligned} \mu &= -\frac{1}{c_1} \\ \frac{dt}{dx} &= -\frac{1}{c_1} \end{aligned} \right\} \quad (6)$$

where $c_1 = \sqrt{\frac{E I_B}{\rho I_1}}$. Then, multiplying equation (4) by dt and using equations (5) yields

$$\frac{1}{c_1} dM + \rho I_1 d\omega - V dt = 0$$

when

$$dt = \frac{1}{c_1} dx$$

Similarly, using equation (6) gives

$$-\frac{1}{c_1} dM + \rho I_1 d\omega - V dt = 0$$

when

$$dt = -\frac{1}{c_1} dx$$

In an analogous fashion, it can be shown, from equations (3b) and (3d), that

$$\frac{1}{c_2} dV - \rho A_1 dv + \left(q + \frac{A_{SG}}{c_2} \omega \right) dt = 0$$

when

$$dt = \frac{1}{c_2} dx$$

and

$$-\frac{1}{c_2} dV - \rho A_1 dv + \left(q - \frac{A_{SG}}{c_2} \omega \right) dt = 0$$

when

$$dt = -\frac{1}{c_2} dx$$

where $c_2 = \sqrt{\frac{A_{SG}}{\rho A_1}}$.

Then, the system of equations (3) has associated with it four real characteristic directions and is thus "totally hyperbolic" (ref. 12). A network of characteristics can readily be constructed without prior knowledge of the unknowns M , V , ω , and v since their slopes depend only on the material and geometrical properties of the beam. For uniform beams, as well as for tapered beams having uniform material properties and geometrically similar cross sections, c_1 and c_2 are constant, and the characteristics will therefore be straight; in general, however,

the characteristics may be curved. Figure 2 illustrates the four characteristics passing through a point P in the space-time plane with the characteristics designated as

$$I+: \quad \frac{dt}{dx} = \frac{1}{c_1}$$

$$I-: \quad \frac{dt}{dx} = -\frac{1}{c_1}$$

$$II+: \quad \frac{dt}{dx} = \frac{1}{c_2}$$

$$II-: \quad \frac{dt}{dx} = -\frac{1}{c_2}$$

It is known that, by virtue of the totally hyperbolic character of the basic equations, the values of the unknowns M , V , ω , and v at the point P depend only on their initial values at $t = 0$ between the points x_1 and x_2 on the beam (ref. 12). Furthermore, these values at P can, in turn, have influence only on points lying in the region above P enveloped by the $I+$ and $I-$ characteristics through P. Thus no signal can proceed along the beam with a velocity greater than c_1 (which is generally larger than c_2 , as illustrated in fig. 2).

For the sake of easy reference, the four characteristic differential forms of the basic equations are grouped below.

$$\text{Along } I+: \quad \frac{1}{c_1} dM + \rho I_1 d\omega - V dt = 0 \quad (7a)$$

$$\text{Along } I-: \quad \frac{1}{c_1} dM - \rho I_1 d\omega + V dt = 0 \quad (7b)$$

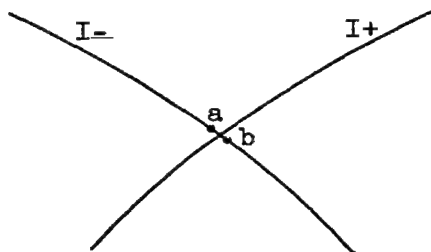
$$\text{Along } II+: \quad \frac{1}{c_2} dV - \rho A_1 dv + (\rho A_1 c_2 \omega + q) dt = 0 \quad (7c)$$

$$\text{Along } II-: \quad \frac{1}{c_2} dV + \rho A_1 dv + (\rho A_1 c_2 \omega - q) dt = 0 \quad (7d)$$

Related forms of these characteristic equations have been written by Robinson (ref. 8) and Pfeiffer (ref. 9).

Propagation of discontinuities.— Characteristics are lines across which discontinuities may exist (ref. 12); indeed, this property is often taken as the basic definition of a characteristic. In the present problem, discontinuities (or jumps) in M and ω can therefore exist across the $I+$ and $I-$ characteristics, and discontinuities in V and v can exist across the $II+$ and $II-$ characteristics. Hence, a jump in M or ω will propagate with the velocity c_1 , whereas a jump in V or v must proceed with the velocity c_2 . It should be remarked that such discontinuities would appear only in the limiting case of a beam subjected to an instantaneous loading. The solution of such idealized problems, which are often instructive, requires a knowledge of the laws governing the variations in strength of these discontinuities as they propagate through the beam. These laws are determined below for nonuniform beams for which it is assumed that the condition $c_1 = c_2$ does not hold over any portion of the beam; in other words, the I and II characteristics are distinct. The special case where $c_1 = c_2$ is considered subsequently when uniform beams are discussed.

Let a and b be two points on a $I-$ characteristic on either side of a particular $I+$ characteristic



If M is discontinuous across the $I+$ characteristic, then $M_a - M_b$ retains a finite value δM as a and b are allowed to approach the $I+$ characteristic from either side. Consequently, from equation (7b) written along the $I-$ characteristic,

$$\frac{1}{c_1} \delta M - \rho I_1 \delta \omega = 0$$

since dt approaches zero as a and b approach each other. Thus, everywhere along a $I+$ characteristic, jumps δM and $\delta \omega$ across this characteristic are related by

$$\delta M = c_1 \rho I_1 \delta \omega \quad (8)$$

Similarly, the jumps across the other characteristics can be readily shown to satisfy

$$\text{Along } I-: \quad \delta M = -c_1 \rho I_1 \delta \omega \quad (9)$$

$$\text{Along } II+: \quad \delta V = -c_2 \rho A_1 \delta v \quad (10)$$

$$\text{Along } II-: \quad \delta V = c_2 \rho A_1 \delta v \quad (11)$$

A jump in M is thus always accompanied by a definite jump in ω ; similarly, jumps in V and v are always coupled together.

The variations in the magnitude of a discontinuity as one proceeds along a characteristic may be determined in the following manner. Equation (7a) is written for the upper side and the lower side of the $I+$ characteristic; then, since V is continuous across a $I+$ characteristic, the difference of the two equations yields

$$d(\delta M) + c_1 \rho I_1 d(\delta \omega) = 0$$

along $I+$. Eliminating $\delta \omega$ by using equation (8) gives

$$d(\delta M) + c_1 \rho I_1 d\left(\frac{\delta M}{c_1 \rho I_1}\right) = 0$$

By carrying out the indicated differentiation in the second term and dividing by $2\delta M$, the following result is obtained:

$$\frac{d(\delta M)}{\delta M} = \frac{1}{2} \frac{d(c_1 \rho I_1)}{c_1 \rho I_1}$$

Solution of this equation gives

$$(\delta M)_2 = (\delta M)_1 \sqrt{\frac{(c_1 \rho I_1)_2}{(c_1 \rho I_1)_1}} \quad (12)$$

as the relationship between the magnitude of the jumps in M at two points 1 and 2 on the $I+$ characteristic.

It can be shown that the identical relationship holds between jumps in M at two points on a I^- characteristic. Similarly, it can be found that, on II^+ and II^- characteristics,

$$(\delta V)_2 = (\delta V)_1 \sqrt{\frac{(c_2 \rho A_1)_2}{(c_2 \rho A_1)_1}} \quad (13)$$

for any two points 1 and 2 on a given characteristic. The corresponding variations of the jumps δw and δv are, of course, readily determined from equations (8) to (11).

Uniform Beams

Nondimensional form of the equations.— The examples to be presented in this report are all concerned with beams having uniform cross-sectional size and shape and uniform material properties throughout their length. For such beams, it is convenient to express Timoshenko's equations in nondimensional form. Thus, equations (3) may be written in terms of

$$\bar{M} = \frac{ML}{EI_B}, \quad \bar{V} = \frac{VL^2}{EI_B}, \quad \bar{w} = \frac{wL}{c_1}, \quad \text{and} \quad \bar{v} = \frac{v}{c_2} \quad \text{as}$$

$$\bar{w}_\xi + \bar{M}_\tau = 0 \quad (14a)$$

$$\frac{c_2}{c_1} \bar{v}_\xi - \frac{1}{R} \bar{V}_\tau - \bar{w} = 0 \quad (14b)$$

$$\bar{M}_\xi + \bar{w}_\tau - \bar{V} = 0 \quad (14c)$$

$$\bar{V}_\xi - R \frac{c_1}{c_2} \bar{v}_\tau + \bar{q} = 0 \quad (14d)$$

where $\xi = \frac{x}{L}$, $\tau = \frac{c_1 t}{L}$, $\bar{q} = \frac{qL^3}{EI_B}$, and $R = \left(\frac{c_2}{c_1}\right)^2 \left(\frac{L}{r_1}\right)^2$. The quantity L refers to the beam length for all beams except those of infinite length, in which case any convenient arbitrary length may be chosen for L .

The characteristics of Timoshenko's equations for a uniform beam are defined in the ξ, τ plane by the families of straight lines

$$I+: \quad \frac{d\tau}{d\xi} = 1 \quad (15a)$$

$$I-: \quad \frac{d\tau}{d\xi} = -1 \quad (15b)$$

$$II+: \quad \frac{d\tau}{d\xi} = \frac{c_1}{c_2} \quad (15c)$$

$$II-: \quad \frac{d\tau}{d\xi} = -\frac{c_1}{c_2} \quad (15d)$$

The nondimensionalized characteristic forms of the basic equations become

$$\text{Along } I+: \quad d\bar{M} + d\bar{\omega} - \bar{V} d\tau = 0 \quad (16a)$$

$$\text{Along } I-: \quad d\bar{M} - d\bar{\omega} + \bar{V} d\tau = 0 \quad (16b)$$

$$\text{Along } II+: \quad d\bar{V} - R d\bar{v} + \left(R\bar{\omega} + \frac{c_2}{c_1} \bar{q} \right) d\tau = 0 \quad (16c)$$

$$\text{Along } II-: \quad d\bar{V} + R d\bar{v} + \left(R\bar{\omega} - \frac{c_2}{c_1} \bar{q} \right) d\tau = 0 \quad (16d)$$

In addition to the restriction to uniform beams, for which c_1 and c_2 are constants, the examples presented herein are further limited to those beams for which the propagation velocities c_1 and c_2 are equal. This assumption has been made because the simplifications that result not only permit the ready attainment of numerical solutions but also, in particular cases, permit the attainment of exact closed solutions for comparison. Since, for this very special case, the characteristics II coincide with the characteristics I, equations (16) may now be written, for $\bar{q} = 0$, as

$$\text{Along } I+: \quad \left\{ \begin{array}{l} d\bar{M} + d\bar{\omega} - \bar{V} d\tau = 0 \\ d\bar{V} - 4\lambda^2 d\bar{v} + 4\lambda^2 \bar{\omega} d\tau = 0 \end{array} \right\} \quad (17a)$$

$$\text{Along } I-: \quad \left\{ \begin{array}{l} d\bar{M} - d\bar{\omega} + \bar{V} d\tau = 0 \\ d\bar{V} + 4\lambda^2 d\bar{v} + 4\lambda^2 \bar{\omega} d\tau = 0 \end{array} \right\} \quad (17b)$$

where $\lambda = \frac{L}{2r_1}$.

Propagation of discontinuities when $c_1 = c_2$. Equations (8) to (13), which describe the behavior of discontinuities in a nonuniform beam, also describe, as a special case, the behavior of discontinuities in a uniform beam for which $c_1 \neq c_2$. They show that such discontinuities propagate with constant magnitude.

However, when the beam has properties such that $c_1 = c_2$, these equations are no longer valid. Equations which are valid in this case may be derived in precisely the same way by using equations (17) instead of equations (7). Discontinuities in such beams can be shown to be related by

$$\text{Along } I+: \quad \left\{ \begin{array}{l} \delta \bar{M} = \delta \bar{w} \\ \delta \bar{V} = -4\lambda^2 \delta \bar{v} \end{array} \right\} \quad (18a)$$

$$\text{Along } I-: \quad \left\{ \begin{array}{l} \delta \bar{M} = -\delta \bar{w} \\ \delta \bar{V} = 4\lambda^2 \delta \bar{v} \end{array} \right\} \quad (18b)$$

as they propagate, and they can be shown to vary in magnitude according to the equations

$$\text{Along } I+ \text{ and } I-: \quad \left\{ \begin{array}{l} \frac{d}{d\tau}(\delta \bar{w}) - \frac{1}{2} \delta \bar{V} = 0 \\ \frac{d}{d\tau}(\delta \bar{V}) + 2\lambda^2 \delta \bar{w} = 0 \end{array} \right\} \quad (19)$$

Equations (19) may be solved simultaneously to obtain

$$\text{Along } I+ \text{ and } I-: \quad \left\{ \begin{array}{l} \delta \bar{w} = A \cos(\lambda\tau - B) \\ \delta \bar{V} = -2\lambda A \sin(\lambda\tau - B) \end{array} \right\} \quad (20)$$

where A and B are arbitrary constants which must be evaluated by using known values of $\delta \bar{w}$ and $\delta \bar{V}$ at some point on the characteristic. The variations in $\delta \bar{M}$ and $\delta \bar{v}$ can then be readily found by using equations (18).

Thus, for the case $c_1 = c_2$, discontinuities in a uniform beam do not propagate unchanged but vary in magnitude sinusoidally as they progress through the beam.

Limitations of the Theory

It may be well to insert a word of caution about the applicability of Timoshenko's theory. The investigations of Prescott (ref. 13) and Cooper (ref. 14) have shown that, when the response of a beam includes components whose wave length is small compared to the depth of the beam, the assumption of Timoshenko's theory that plane sections remain plane after bending is, as might be expected, too restrictive. Since applied disturbances which could give rise to discontinuities would obviously excite even the shortest wave length in the spectrum of the response, the results obtained by application of Timoshenko's theory to such hypothetical problems cannot, in themselves, have practical significance. However, carrying out solutions involving discontinuities is a useful means of testing methods of solution of the Timoshenko equations with a view to applying these methods to problems in which discontinuities do not exist. Furthermore, the admittedly inaccurate response to an infinitely abrupt disturbance may be used to obtain the correct response to disturbances of a more practical nature through the application of Duhamel's superposition integral.

SPECIFIC EXAMPLES - FINITE UNIFORM BEAMS WITH $c_1 = c_2$

Three specific examples are considered; they are: a cantilever beam given a step velocity at the root, a simply supported beam subjected to a step moment at one end, and a simply supported beam subjected to a ramp-platform moment at one end.

Methods of Solution

In the examples, the results of calculation by the following three methods are compared: (a) numerical step-by-step integration along the characteristics, (b) normal-mode superposition, and (c) exact closed-form solution. The first two procedures are approximate in character, but they could conceivably be generalized sufficiently to be applied to practical structures; the last procedure, although exact, would rarely be useful in practice and is introduced herein chiefly as a check on the accuracy of the first two.

The detailed descriptions and applications of the three methods are contained in appendixes A, B, and C. In brief, the numerical procedure exploits a grid of characteristic lines as shown in figure 3(a). For

the case $c_1 = c_2$ that is under consideration, this grid consists of two families of lines in the ξ, τ plane with slopes 1 and -1. A recurrence formula is developed in appendix A that gives the values of \bar{u} and \bar{v} at station 1 of a typical interior mesh (see fig. 3(b)) in terms of the values of \bar{u} and \bar{v} at stations 2, 3, and 4. Repeated application of this formula, together with the use of special formulas for the half-meshes at either end of the beam and the knowledge of the magnitudes of jumps in \bar{u} and \bar{v} across characteristics where they occur, permits \bar{u} and \bar{v} to be calculated throughout the ξ, τ plane. Subsequent determination of \bar{M} and \bar{V} is achieved by means of simple addition formulas utilizing these calculated values of \bar{u} and \bar{v} .

Although the solutions derived in appendix B have actually been obtained by Laplace transform techniques, they have been termed "modal solutions" because they are exactly those which would result from an application of the usual mode-superposition process. The exact closed solutions in appendix C have also been obtained through the use of Laplace transforms.

Cantilever Beam Given a Step Velocity at the Root

The first example to be considered, the response of a uniform cantilever beam given a step velocity $\bar{v} = 1$ at the root, is the equivalent of the most severe idealized landing problem, the instantaneous arrest of the root of a moving cantilever beam. Computed results for the shear and moment at the root of such a beam having a ratio of length to radius of gyration of 10 ($\lambda = 5$) and properties such that $c_1 = c_2$ are presented in figures 4(a) and 4(b), respectively. Two separate curves obtained by the numerical procedure are shown - one from a grid that divides the beam into 10 segments and the other from a 20-segment solution. The modal solution includes the contributions of the first eight modes. Results given by an exact closed solution are shown for both the shear and moment at the root up to the time $\tau = 2$. These exact results are actually those for an infinitely long beam, since the influence of the free end is not felt at the root until $\tau = 2$. After $\tau = 2$, the influence of the free end is felt and, in this case, an exact solution is not feasible. To illustrate the time range covered in the plots, the point corresponding to half the period of the first mode of vibration of the beam is indicated on the time scale of each plot.

In figure 4(a), the shear discontinuities evident in the numerical solutions occur each time the discontinuous wave front returns to the root after being reflected at the free end. The beam is seen to react violently to each of these boosts by the wave front, with more and more

oscillations occurring after each succeeding jump. The frequency of these oscillations tends to increase with each succeeding boost until limited by the finite time interval. In these regions of violent oscillation the accuracy of the numerical solutions is obviously questionable; indeed the question arises as to whether these oscillations are really predicted by the theory or are merely the result of some instability in the numerical process. This question is resolved in the next section in which the simply supported beam is considered. At any rate, away from the regions of violent oscillations, the comparisons with the modal solution are favorable, and, for $\tau < 2$, the fine-grid numerical solution almost coincides with the exact closed solution valid in this region.

The comparisons between the numerical and modal solutions are very good in figure 4(b) where the time history of the moment at the root is plotted. Again, the fine-grid numerical solution nearly coincides with the exact closed solution for $\tau < 2$.

Simply Supported Beam With an Applied End Moment

Step moment.— A simply supported uniform beam with a ratio of length to radius of gyration of 10 ($\lambda = 5$) and properties such that $c_1 = c_2$ is subjected to a step moment $\bar{M} = 1$ at the end $\xi = 0$. Computed results for the shear at $\xi = 0$ are presented in figure 5(a) and the time history of moment at the center of the beam is presented in figure 5(b). The point corresponding to the full period of the first mode is marked on the time scale of each plot. The numerical curves for both shear and moment were obtained by a 20-segment solution. The modal curves were obtained by adding dynamic corrections to the static solutions, the dynamic corrections being calculated with six modes for both the shear and the moment.

This example affords an answer to the question raised in the preceding section with regard to the stability of the numerical procedure following the passage of a discontinuous wave front. The fact is that the violent oscillations that occur after the discontinuity actually appear in the exact solution (fig. 5(a)) and are hence inherently present in the theory.

In figure 5(a) the scale of dimensionless vertical shear happens to be precisely the dynamic overshoot factor; it is of interest to note that values at least 15 times the static shear are predicted when the moment is applied suddenly.

For shear (fig. 5(a)), the inaccuracies in the numerical solution just after the discontinuities are evident; however, the numerical results approximate the exact solution very well elsewhere. A similar

observation may be made for the modal solution, which, as would be expected, ignores the discontinuities and violent oscillations caused by the wave front. The numerical and modal curves for the moment in figure 5(b) follow the same pattern, agreeing well everywhere except in the regions immediately following the discontinuities.

Ramp-platform moment.- Computed results for the shear at the end $\xi = 0$ and the moment at the center of the same simply supported uniform beam subjected to the applied ramp-platform moment

$$\bar{M}(0, \tau) = \tau \quad (0 \leq \tau \leq 1)$$

$$\bar{M}(0, \tau) = 1 \quad (\tau > 1)$$

are presented in figures 6(a) and 6(b). Again, the period of the first mode of vibration is marked on the time scales.

The numerical curves were recomputed with a 20-segment grid for the new forcing function; however, the results for the modal and exact solutions were obtained by means of a superposition of the preceding results. This superposition was carried out analytically for the complete modal solution and for the exact solution in the range $\tau < 2$. In the range $\tau > 2$, it was necessary to carry out the superposition for the exact solution numerically.

In figure 6 the time to peak value of the applied moment is seen to be approximately one-seventh the period of the first mode; predicted shear values approximately three and one-half times the static response occur.

With the removal of the discontinuity, there remain no high-frequency oscillations which the numerical solution might be unable to represent. In fact, all three solutions for the shear and both moment solutions are seen to be in excellent agreement.

CONCLUDING REMARKS

Timoshenko's equations for the motion of vibrating nonuniform beams may be written in a characteristic form which appears to be well-suited to solution by numerical methods. In the examples presented in this report, all of which are for uniform beams with equal propagation velocities of bending and shear discontinuities ($c_1 = c_2$), the solutions by the

numerical and modal methods generally agree well with each other as well as with exact closed solutions where these have been obtained. However, the modal method, of course, fails entirely to reproduce discontinuities in shear or moment, and the numerical procedure, although it yields these discontinuities, does so with decreasing accuracy as more and more reflections of the wave front occur. In the more practical situations where discontinuities do not exist, these difficulties will, of course, not arise.

The results of the examples carried out by the numerical traveling-wave procedure encourage the viewpoint that such traveling-wave analyses may eventually be of practical usefulness. This kind of procedure is inherently simple and straightforward and has the advantage that the bulk of the labor involved is routine computation rather than mathematical analysis. It should be emphasized, however, that numerical solutions of Timoshenko's equations have been demonstrated only for uniform beams in which the propagation velocities c_1 and c_2 are equal; numerical procedures for the general case where they are unequal remain to be developed and tested.

Langley Aeronautical Laboratory,
National Advisory Committee for Aeronautics,
Langley Field, Va., October 28, 1952.

APPENDIX A

NUMERICAL SOLUTIONS FOR UNIFORM BEAMS WITH $c_1 = c_2$

Matrix Formulation

Let the differential equations (17) be replaced by the finite-difference equations

$$\text{Along } I+: \quad \begin{cases} \Delta \bar{M} + \Delta \bar{\omega} - \bar{V} \Delta \tau = 0 & (\text{A1a}) \\ \Delta \bar{V} - 4\lambda^2 \Delta \bar{V} + 4\lambda^2 \bar{\omega} \Delta \tau = 0 & (\text{A1b}) \end{cases}$$

$$\text{Along } I-: \quad \begin{cases} \Delta \bar{M} - \Delta \bar{\omega} + \bar{V} \Delta \tau = 0 & (\text{A1c}) \\ \Delta \bar{V} + 4\lambda^2 \Delta \bar{V} + 4\lambda^2 \bar{\omega} \Delta \tau = 0 & (\text{A1d}) \end{cases}$$

and consider a closely spaced network of $I+$ and $I-$ characteristics in the space-time plane as shown in figure 3(a). Let the corners of a typical interior mesh of this grid be designated as shown in figure 3(b). A step-by-step integration formula for $\bar{\omega}$ and \bar{V} may now be derived in the following manner.

Equations (A1) may be written along the upper sides of the typical mesh to obtain

$$\bar{M}_1 - \bar{M}_2 + \bar{\omega}_1 - \bar{\omega}_2 - \frac{\Delta \tau}{2}(\bar{V}_1 + \bar{V}_2) = 0 \quad (\text{A2})$$

$$\bar{M}_1 - \bar{M}_3 - \bar{\omega}_1 + \bar{\omega}_3 + \frac{\Delta \tau}{2}(\bar{V}_1 + \bar{V}_3) = 0 \quad (\text{A3})$$

$$\bar{V}_1 - \bar{V}_2 - 4\lambda^2(\bar{V}_1 - \bar{V}_2) + 2\lambda^2 \Delta \tau (\bar{\omega}_1 + \bar{\omega}_2) = 0 \quad (\text{A4})$$

$$\bar{V}_1 - \bar{V}_3 + 4\lambda^2(\bar{V}_1 - \bar{V}_3) + 2\lambda^2 \Delta \tau (\bar{\omega}_1 + \bar{\omega}_3) = 0 \quad (\text{A5})$$

where $\bar{\omega}$ and \bar{V} have been assumed to vary linearly in the small intervals between the corners. Obviously equations (A2) to (A5) may be solved simultaneously to obtain the four quantities \bar{V} , $\bar{\omega}$, \bar{V} , and \bar{M}

at point 1 in terms of their values at points 2 and 3. However, it is noted that, if \bar{V} , $\bar{\omega}$, \bar{v} , and \bar{M} at points 2 and 3 were determined by a similar process for the preceding meshes, they already satisfy the equations

$$\bar{M}_2 - \bar{M}_4 - \bar{\omega}_2 + \bar{\omega}_4 + \frac{\Delta\tau}{2}(\bar{v}_2 + \bar{v}_4) = 0 \quad (A6)$$

$$\bar{M}_3 - \bar{M}_4 + \bar{\omega}_3 - \bar{\omega}_4 - \frac{\Delta\tau}{2}(\bar{v}_3 + \bar{v}_4) = 0 \quad (A7)$$

$$\bar{v}_2 - \bar{v}_4 + 4\lambda^2(\bar{v}_2 - \bar{v}_4) + 2\lambda^2\Delta\tau(\bar{\omega}_2 + \bar{\omega}_4) = 0 \quad (A8)$$

$$\bar{v}_3 - \bar{v}_4 - 4\lambda^2(\bar{v}_3 - \bar{v}_4) + 2\lambda^2\Delta\tau(\bar{\omega}_3 + \bar{\omega}_4) = 0 \quad (A9)$$

Equations (A6) and (A7) may be added to equations (A2) and (A3), respectively, to obtain

$$\bar{M}_1 - \bar{M}_4 + \bar{\omega}_1 - 2\bar{\omega}_2 + \bar{\omega}_4 - \frac{\Delta\tau}{2}(\bar{v}_1 - \bar{v}_4) = 0$$

and

$$\bar{M}_1 - \bar{M}_4 - \bar{\omega}_1 + 2\bar{\omega}_3 - \bar{\omega}_4 + \frac{\Delta\tau}{2}(\bar{v}_1 - \bar{v}_4) = 0$$

which may, in turn, be subtracted to obtain the single equation

$$\bar{\omega}_1 - \bar{\omega}_2 - \bar{\omega}_3 + \bar{\omega}_4 - \frac{\Delta\tau}{2}(\bar{v}_1 - \bar{v}_4) = 0 \quad (A10)$$

Similarly, equations (A8) and (A9) may be subtracted from equations (A4) and (A5), respectively, to obtain

$$\bar{v}_1 - 2\bar{v}_2 + \bar{v}_4 - 4\lambda^2(\bar{v}_1 - \bar{v}_4) + 2\lambda^2\Delta\tau(\bar{\omega}_1 - \bar{\omega}_4) = 0$$

and

$$\bar{v}_1 - 2\bar{v}_3 + \bar{v}_4 + 4\lambda^2(\bar{v}_1 - \bar{v}_4) + 2\lambda^2\Delta\tau(\bar{\omega}_1 - \bar{\omega}_4) = 0$$

and these may be added to derive

$$\bar{V}_1 - \bar{V}_2 - \bar{V}_3 + \bar{V}_4 + 2\lambda^2 \Delta\tau (\bar{\omega}_1 - \bar{\omega}_4) = 0 \quad (A11)$$

Equations (A10) and (A11) may now be solved simultaneously to obtain the step-by-step integration formula

$$\begin{bmatrix} \bar{\omega}_1 \\ \bar{V}_1 \end{bmatrix} = \frac{1}{(\lambda \Delta\tau)^2 + 1} \left\{ \begin{bmatrix} \Lambda_{23} \end{bmatrix} \begin{bmatrix} \bar{\omega}_2 + \bar{\omega}_3 \\ \bar{V}_2 + \bar{V}_3 \end{bmatrix} + \begin{bmatrix} \Lambda_{14} \end{bmatrix} \begin{bmatrix} \bar{\omega}_4 \\ \bar{V}_4 \end{bmatrix} \right\} \quad (A12)$$

where

$$\begin{bmatrix} \Lambda_{23} \end{bmatrix} = \begin{bmatrix} 1 & \frac{\Delta\tau}{2} \\ -2\lambda^2 \Delta\tau & 1 \end{bmatrix}$$

and

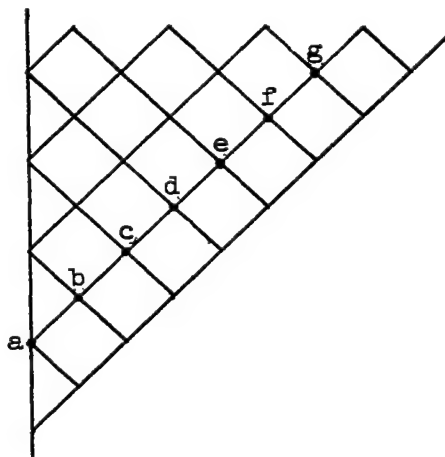
$$\begin{bmatrix} \Lambda_{14} \end{bmatrix} = \begin{bmatrix} (\lambda \Delta\tau)^2 - 1 & -\Delta\tau \\ 4\lambda^2 \Delta\tau & (\lambda \Delta\tau)^2 - 1 \end{bmatrix}$$

Thus $\bar{\omega}$ and \bar{V} may be determined at every interior mesh point in the space-time plane by the repeated application of formula (A12) to each mesh as it is encountered. The half-meshes which occur at the vertical left and right boundaries of the plane (fig. 3(a)) require special formulas incorporating the known boundary data. These formulas may be derived from equations (A1) by a procedure similar to that used in obtaining equation (A12). Boundary formulas for some specific examples are presented in subsequent sections of this appendix.

Besides boundary data, initial data must be provided in order that a step-by-step solution may be begun. In all the examples considered, the beam is initially at rest and has a disturbance applied at the point $\xi = 0$ beginning at time $\tau = 0$. The region $\tau < \xi$ (without grid lines in fig. 3(a)) therefore is one of zero stress and motion and $\bar{\omega}$ and \bar{V} are given along the line $\tau = \xi$ by the known conditions at the wave front. It is with these values that each numerical solution is begun.

Discontinuities in $\bar{\omega}$ and \bar{v} offer no special difficulties since they propagate so as to be always located on I characteristics which, of course, can be made part of the basic grid. Thus they are simply added as they are encountered.

Once $\bar{\omega}$ and \bar{v} have been determined at the grid intersections by the step-by-step process, \bar{M} and \bar{v} may be found by repeated application of equation (A2) or (A3) and equation (A4) or (A5) along the proper grid lines from boundaries where \bar{M} and \bar{v} are known. For example, if \bar{M} is known along the left boundary, it may be found at a point g



by applying equation (A2) successively to the intervals ab, bc, cd, . . . fg. The resulting expression for \bar{M}_g becomes

$$\bar{M}_g = \bar{M}_a + \bar{\omega}_a - \bar{\omega}_g + \Delta\tau \left(\frac{1}{2} \bar{v}_a + \bar{v}_b + \dots + \bar{v}_f + \frac{1}{2} \bar{v}_g \right) \quad (A13)$$

This procedure is seen to correspond to integration of the first of differential equations (17a) by means of the trapezoidal rule.

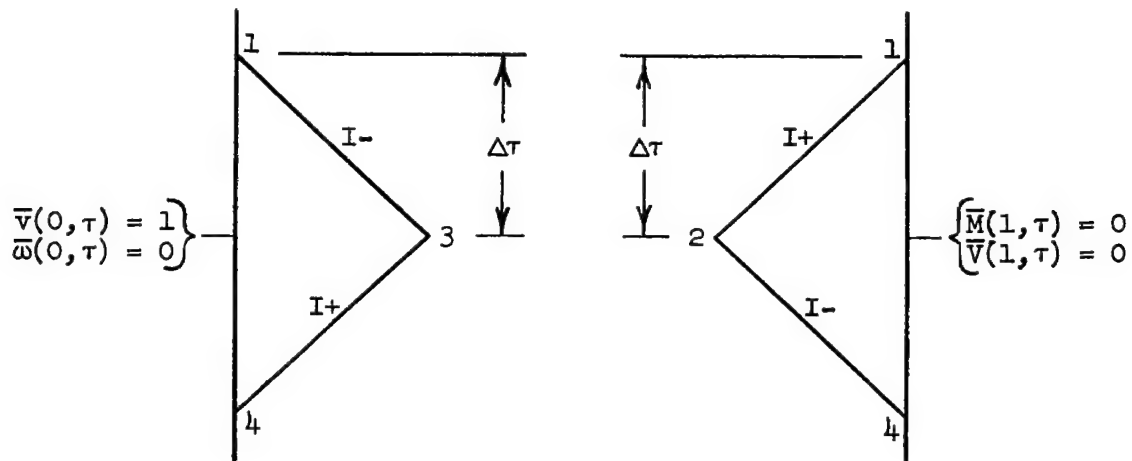
Specific Problems

Cantilever beam given a step velocity at the root.- If the root $\xi = 0$ of a uniform cantilever beam is given a step velocity $\bar{v} = 1$

at time $\tau = 0$, the boundary conditions may be written

$$\left. \begin{aligned} \bar{v}(0, \tau) &= 1 \\ \bar{\omega}(0, \tau) &= 0 \\ \bar{M}(1, \tau) &= 0 \\ \bar{V}(1, \tau) &= 0 \end{aligned} \right\} \quad (A14)$$

Typical left- and right-boundary half-meshes are



Application of equations (Alb) and (Ald) to the sides of the left-boundary half-mesh and proper combination of the resulting equations to eliminate \bar{v} produces

$$\bar{v}_1 = 2\bar{v}_3 - \bar{v}_4 \quad (A15)$$

Similarly, application of equations (Ala) and (Alc) to a right-boundary half-mesh produces

$$\bar{\omega}_1 = 2\bar{\omega}_2 - \bar{\omega}_4 \quad (A16)$$

so that a complete set of integration formulas for determining $\bar{\omega}$ and \bar{v} for this problem is now available. In addition, if the unused equations (eqs. (Ala) and (Alc) for the left-boundary half-mesh and eqs. (Alb) and (Ald) for the right) are applied and combined to eliminate \bar{M} and \bar{V}

at points 3 and 2, the recurrence relations

$$\bar{M}_1 = \bar{M}_4 - 2\bar{\omega}_3 - \frac{\Delta\tau}{2}(\bar{V}_1 - \bar{V}_4) \quad (A17)$$

for left-boundary half-meshes and

$$\bar{V}_1 = \bar{V}_4 - \frac{1}{2\lambda^2} \bar{V}_2 + \frac{\Delta\tau}{2}(\bar{\omega}_1 - \bar{\omega}_4) \quad (A18)$$

for right-boundary half-meshes are obtained. These equations may be used to compute \bar{M} at the root and \bar{V} at the tip after $\bar{\omega}$ and \bar{V} have been determined everywhere.

Since the applied disturbance is initially discontinuous, $\bar{\omega}$ and \bar{V} will be discontinuous along the line $\tau = \xi$ (see fig. 3(a)). In order to begin the step-by-step solution for $\bar{\omega}$ and \bar{V} , these discontinuities must be determined in advance. Furthermore, since the wave front is reflected back into the beam at either end, $\bar{\omega}$ and \bar{V} will also be discontinuous along the lines $\tau = 2 - \xi$, $\tau = 2 + \xi$, . . ., and $\delta\bar{\omega}$ and $\delta\bar{V}$ must be determined along each of these lines before the step-by-step solution can be extended beyond it. The discontinuities at the wave front are determined as follows.

From the boundary conditions (A14), it is seen that $\delta\bar{\omega}(0,0) = 0$ and $\delta\bar{V}(0,0) = 1$. Thus, from equation (18a), $\delta\bar{V}(0,0) = -4\lambda^2$, and equations (20) become, for the line $\tau = \xi$,

$$\left. \begin{aligned} \delta\bar{\omega}(\xi, \xi) &= -2\lambda \sin \lambda \xi \\ \delta\bar{V}(\xi, \xi) &= -4\lambda^2 \cos \lambda \xi \end{aligned} \right\} \quad (A19)$$

At $\xi = 1$, the discontinuities across $\tau = \xi$ are $\delta\bar{\omega}(1,1) = \delta\bar{M}(1,1) = -2\lambda \sin \lambda$ and $\delta\bar{V}(1,1) = -4\lambda^2 \cos \lambda$, so that, if the boundary conditions $\bar{M}(1,\tau) = \bar{V}(1,\tau) = 0$ are to be satisfied, jumps must occur across $\tau = 2 - \xi$ at the point (1,1) with the magnitudes $\delta\bar{\omega}(1,1) = -\delta\bar{M}(1,1) = -2\lambda \sin \lambda$ and $\delta\bar{V}(1,1) = 4\lambda^2 \cos \lambda$. In view of these initial conditions at $\tau = 1$, equations (20) become, for the line $\tau = 2 - \xi$,

$$\left. \begin{aligned} \delta\bar{\omega}(\xi, 2-\xi) &= -2\lambda \sin \lambda \xi \\ \delta\bar{V}(\xi, 2-\xi) &= 4\lambda^2 \cos \lambda \xi \end{aligned} \right\} \quad (A20)$$

Initial jump values $\delta\bar{\omega}(0,2) = 0$ and $\delta\bar{V}(0,2) = 4\lambda^2$ for the line $\tau = 2 + \xi$ may be found from equation (A20) by satisfying the boundary conditions $\bar{\omega}(0,\tau) = 0$ and $\bar{V}(0,\tau) = 1$. From these initial values, the discontinuities across $\tau = 2 + \xi$ are found to be the negative of those across $\tau = \xi$, or

$$\left. \begin{aligned} \delta\bar{\omega}(\xi, 2+\xi) &= 2\lambda \sin \lambda \xi \\ \delta\bar{V}(\xi, 2+\xi) &= 4\lambda^2 \cos \lambda \xi \end{aligned} \right\} \quad (A21)$$

Then, it must be true that

$$\left. \begin{aligned} \delta\bar{\omega}(\xi, 4-\xi) &= 2\lambda \sin \lambda \xi \\ \delta\bar{V}(\xi, 4-\xi) &= -4\lambda^2 \cos \lambda \xi \end{aligned} \right\} \quad (A22)$$

and so forth, with the values on each succeeding line $\tau = n \pm \xi$ repeating the values on the line $\tau = (n - 4) \pm \xi$. The variations in the magnitudes of $\delta\bar{\omega}$ and $\delta\bar{V}$ as the wave front propagates back and forth through the beam are thus clearly defined, and, since $\tau < \xi$ is a region of zero stress and motion, equations (A19) define the values of $\bar{\omega}$ and \bar{V} along the line $\tau = \xi$.

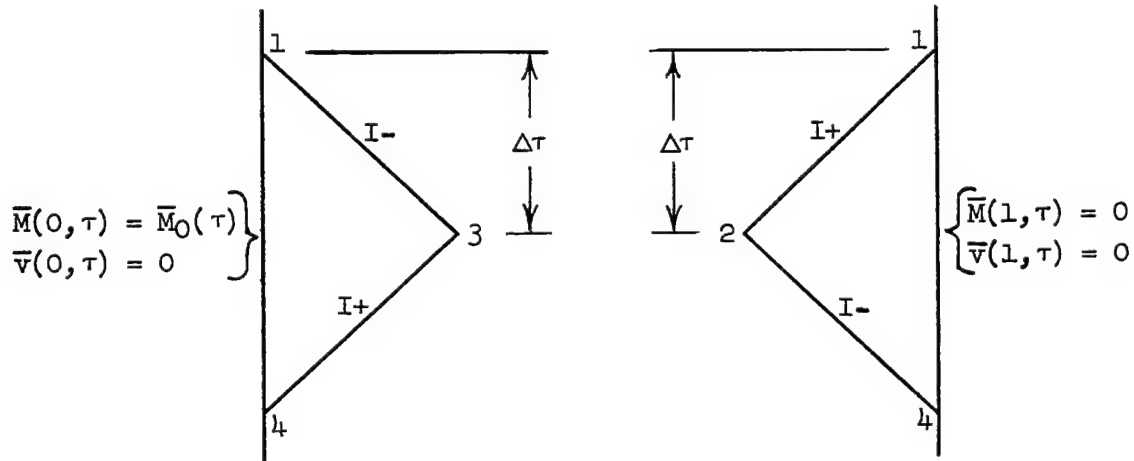
With $\bar{\omega}$ and \bar{V} known along $\tau = \xi$, the solution for $\bar{\omega}$ and \bar{V} may be begun by applying formula (A15) to the half-mesh in the lower corner of triangular region ① (fig. 3(a)). It is continued step by step throughout the triangle, with formula (A12) being used for all interior meshes. When the first triangle is complete, the known jumps along the line $\tau = 2 - \xi$ may be added to the values computed for the under side of this line, and the solution may then be carried out in triangle ② beginning again at the lower corner this time with formula (A16). In this way the solution may be carried through as many triangular regions as desired.

Two sets of computations, with time intervals $\Delta\tau = 0.1$ and $\Delta\tau = 0.05$, have been made for a cantilever beam for which $\lambda = 5$. These time intervals correspond to grids dividing the beam into 10 and 20 segments, respectively. (The computations for the 20-segment solution were made on the Bell Telephone Laboratories X-66744 relay computer at the Langley Laboratory.) The computed time histories of shear and moment at the root have been plotted in figures 4(a) and 4(b), respectively, up to $\tau = 10$. In order to obtain these time histories, the computations for $\bar{\omega}$ and \bar{V} had to be carried through the first nine triangular regions.

Simply supported beam with an applied end moment.- If the end $\xi = 0$ of a uniform simply supported beam for which $c_1 = c_2$ is subjected to an applied bending moment $\bar{M}_0(\tau)$ beginning at time $\tau = 0$, the boundary conditions are

$$\left. \begin{aligned} \bar{M}(0, \tau) &= \bar{M}_0(\tau) \\ \bar{v}(0, \tau) &= 0 \\ \bar{M}(1, \tau) &= 0 \\ \bar{v}(1, \tau) &= 0 \end{aligned} \right\} \quad (A23)$$

Typical left- and right-boundary half-meshes for this beam are



Equations (A1c), (A1a), (A1d), and (A1b) may be written along the sides of the left half-mesh to give, respectively,

$$(\bar{M}_0)_1 - \bar{M}_3 - \bar{\omega}_1 + \bar{\omega}_3 + \frac{\Delta\tau}{2}(\bar{v}_1 + \bar{v}_3) = 0$$

$$\bar{M}_3 - (\bar{M}_0)_4 + \bar{\omega}_3 - \bar{\omega}_4 - \frac{\Delta\tau}{2}(\bar{v}_3 + \bar{v}_4) = 0$$

$$\bar{v}_1 - \bar{v}_3 - 4\lambda^2\bar{v}_3 + 2\lambda^2\Delta\tau(\bar{\omega}_1 + \bar{\omega}_3) = 0$$

$$\bar{v}_3 - \bar{v}_4 - 4\lambda^2\bar{v}_3 + 2\lambda^2\Delta\tau(\bar{\omega}_3 + \bar{\omega}_4) = 0$$

Adding the first two equations and subtracting the last two equations produces

$$(\bar{M}_0)_1 - (\bar{M}_0)_4 - \bar{\omega}_1 + 2\bar{\omega}_3 - \bar{\omega}_4 + \frac{\Delta\tau}{2}(\bar{v}_1 - \bar{v}_4) = 0$$

and

$$\bar{v}_1 - 2\bar{v}_3 + \bar{v}_4 + 2\lambda^2\Delta\tau(\bar{\omega}_1 - \bar{\omega}_4) = 0$$

which may be solved simultaneously for $\bar{\omega}_1$ and \bar{v}_1 to obtain

$$\begin{vmatrix} \bar{\omega}_1 \\ \bar{v}_1 \end{vmatrix} = \frac{1}{(\lambda \Delta\tau)^2 + 1} \left\{ \begin{bmatrix} \Lambda_{23} \\ \Lambda_4 \end{bmatrix} \begin{vmatrix} 2\bar{\omega}_3 \\ 2\bar{v}_3 \end{vmatrix} + \begin{bmatrix} \Lambda_{23} \\ \Lambda_4 \end{bmatrix} \begin{vmatrix} \bar{\omega}_4 \\ \bar{v}_4 \end{vmatrix} + \left((\bar{M}_0)_1 - (\bar{M}_0)_4 \right) \begin{vmatrix} 1 \\ -2\lambda^2\Delta\tau \end{vmatrix} \right\} \quad (A24)$$

where $[\Lambda_{23}]$ and $[\Lambda_4]$ have been defined in conjunction with equation (A12).

A similar process produces, for the right-boundary half-mesh, the formula

$$\begin{vmatrix} \bar{\omega}_1 \\ \bar{v}_1 \end{vmatrix} = \frac{1}{(\lambda \Delta\tau)^2 + 1} \left\{ \begin{bmatrix} \Lambda_{23} \\ \Lambda_4 \end{bmatrix} \begin{vmatrix} 2\bar{\omega}_2 \\ 2\bar{v}_2 \end{vmatrix} + \begin{bmatrix} \Lambda_{23} \\ \Lambda_4 \end{bmatrix} \begin{vmatrix} \bar{\omega}_4 \\ \bar{v}_4 \end{vmatrix} \right\} \quad (A25)$$

Now consider the case in which the applied moment is a step moment; that is, $\bar{M}_0(\tau) = 1$. Equation (A24) reduces to

$$\begin{vmatrix} \bar{\omega}_1 \\ \bar{v}_1 \end{vmatrix} = \frac{1}{(\lambda \Delta\tau)^2 + 1} \left\{ \begin{bmatrix} \Lambda_{23} \\ \Lambda_4 \end{bmatrix} \begin{vmatrix} 2\bar{\omega}_3 \\ 2\bar{v}_3 \end{vmatrix} + \begin{bmatrix} \Lambda_{23} \\ \Lambda_4 \end{bmatrix} \begin{vmatrix} \bar{\omega}_4 \\ \bar{v}_4 \end{vmatrix} \right\} \quad (A26)$$

for left-boundary half-meshes. A similarity between the boundary formulas (A25) and (A26) and the interior formula (A12) is apparent; indeed, formula (A12) may be used everywhere if the sums of the values at points 2 and 3 are simply replaced by twice the values at the inboard point of each boundary mesh.

For this problem, as in the preceding one, the magnitudes of the discontinuities $\delta\bar{\omega}$ and $\delta\bar{V}$ at the wave front must be determined in advance for every point on the grid lines defining its position. From the boundary conditions and equations (18a) it is apparent that $\delta\bar{\omega}(0,0) = \delta\bar{M}(0,0) = 1$ and $\delta\bar{V}(0,0) = 0$. Thus, for the line $\tau = \xi$, equations (20) become

$$\left. \begin{aligned} \delta\bar{\omega} &= \cos \lambda \tau \\ \delta\bar{V} &= -2\lambda \sin \lambda \tau \end{aligned} \right\} \quad (A27)$$

Furthermore, it is found that, when the wave front is reflected at either of the simply supported ends, the signs as well as the magnitudes of the discontinuities remain unchanged, in contrast to the behavior of a discontinuous wave front reflected at a free or fixed end as in the preceding case. Thus equation (A27) must be valid for the entire zigzag path defining the position of the wave front.

With the discontinuities known, the step-by-step solution can be begun as before. Again, it is convenient to complete each triangular region before proceeding to the next.

Computations for this problem were made on the Bell computer, with a 20-segment grid, for a beam with $\lambda = 5$. The quantities $\bar{\omega}$ and \bar{V} were found in the first eight triangular regions; in addition, the moment at the center was computed. The time histories of shear at the end $\xi = 0$ and of moment at the center $\xi = \frac{1}{2}$ have been plotted in figures 5(a) and 5(b), respectively.

Now consider the case in which a ramp-platform moment is applied to the beam; that is, $\bar{M}_0(\tau)$ is defined by

$$\left. \begin{aligned} \bar{M}_0(\tau) &= \tau & (0 \leq \tau \leq 1) \\ \bar{M}_0(\tau) &= 1 & (\tau > 1) \end{aligned} \right\} \quad (A28)$$

Equation (A24) reduces to

$$\begin{vmatrix} \bar{\omega}_1 \\ \bar{V}_1 \end{vmatrix} = \frac{1}{(\lambda \Delta\tau)^2 + 1} \left\{ \begin{bmatrix} \Lambda_{23} \end{bmatrix} \begin{vmatrix} 2\bar{\omega}_3 \\ 2\bar{V}_3 \end{vmatrix} + \begin{bmatrix} \Lambda_{14} \end{bmatrix} \begin{vmatrix} \bar{\omega}_4 \\ \bar{V}_4 \end{vmatrix} + 2 \Delta\tau \begin{vmatrix} 1 \\ -2\lambda^2 \Delta\tau \end{vmatrix} \right\} \quad (A29)$$

for the left-boundary half-meshes for which $\tau_1 \leq 1$ and reduces to equation (A26) for all the rest. Equations (A12) and (A25) are, of course, still valid for interior meshes and right-boundary half-meshes, respectively.

Since $\delta\bar{\omega}(0,0) = \delta\bar{V}(0,0) = 0$ for this case, the solution begins with initial values $\bar{\omega} = \bar{V} = 0$ along the line $\tau = \xi$ and there are no discontinuities to be added. Thus the solution may progress in any convenient manner without regard for the position of the wave front.

The same quantities were computed for this problem that were obtained in the preceding case. As before, it was assumed that $\lambda = 5$, and the calculations were performed on the Bell computer with a 20-segment grid.

The resulting time histories of shear at $\xi = 0$ and moment at $\xi = \frac{1}{2}$ are presented in figures 6(a) and 6(b), respectively.

APPENDIX B

MODAL SOLUTIONS FOR UNIFORM BEAMS

The solutions carried out in this and the following appendix make considerable use of Laplace transform techniques; all the Laplace transforms used, most of which were taken directly from references 15 and 16, are given in table I for the sake of easy reference.

Equations

The equations of motion (2) may be written for a uniform beam vibrating in the absence of external distributed loading in nondimensional form as

$$\left. \begin{aligned} (\bar{y}_{\xi} - \psi)_{\xi} - \left(\frac{c_1}{c_2}\right)^2 \bar{y}_{\tau\tau} &= 0 \\ \psi_{\xi\xi} + R(\bar{y}_{\xi} - \psi) - \psi_{\tau\tau} &= 0 \end{aligned} \right\} \quad (B1)$$

where $\bar{y} = \frac{Y}{L}$. The dimensionless bending moment \bar{M} and vertical shear \bar{V} are given by (see eqs. (1))

$$\bar{M} = -\psi_{\xi} \quad (B2)$$

$$\bar{V} = R(\bar{y}_{\xi} - \psi) \quad (B3)$$

If the beam is initially at rest ($\bar{y}(\xi, 0) = \bar{y}_{\tau}(\xi, 0) = \psi(\xi, 0) = \psi_{\tau}(\xi, 0) = 0$), equations (B1) may be transformed to (where transform 6 in table I has been used)

$$\left. \begin{aligned} (Y_{\xi} - \Psi)_{\xi} - \left(\frac{c_1}{c_2}\right)^2 p^2 Y &= 0 \\ \Psi_{\xi\xi} + R(Y_{\xi} - \Psi) - p^2 \Psi &= 0 \end{aligned} \right\} \quad (B4)$$

in terms of the Laplace transforms $Y(\xi, p) = \int_0^\infty e^{-p\tau} \bar{y}(\xi, \tau) d\tau$ and $\Psi(\xi, p) = \int_0^\infty e^{-p\tau} \psi(\xi, \tau) d\tau$. The solutions of equations (B4) have the form

$$\left. \begin{aligned} Y(\xi, p) &= A(p) e^{m\xi} \\ \Psi(\xi, p) &= B(p) e^{m\xi} \end{aligned} \right\} \quad (B5)$$

Substituting these relations into equations (B4) leads to a biquadratic equation in m

$$m^4 - p^2 \left[1 + \left(\frac{c_1}{c_2} \right)^2 \right] m^2 + \left(\frac{c_1}{c_2} \right)^2 p^2 (p^2 + R) = 0 \quad (B6)$$

and gives the following relationship between B and A :

$$B = \frac{m^2 - \left(\frac{c_1}{c_2} \right)^2 p^2}{m} A \quad (B7)$$

Let the solutions of equation (B6) be written $m = \pm im_1$ and $\pm im_2$. Then

$$m_1 = p \sqrt{\frac{-\left[1 + \left(\frac{c_1}{c_2} \right)^2 \right] + \sqrt{\left[1 - \left(\frac{c_1}{c_2} \right)^2 \right]^2 - \frac{4R}{p^2} \left(\frac{c_1}{c_2} \right)^2}}{2}}$$

$$m_2 = p \sqrt{\frac{1 + \left(\frac{c_1}{c_2} \right)^2 + \sqrt{\left[1 - \left(\frac{c_1}{c_2} \right)^2 \right]^2 - \frac{4R}{p^2} \left(\frac{c_1}{c_2} \right)^2}}{2}}$$

and the general solution of equations (B4) is

$$Y(\xi, p) = C_1 \cos m_1 \xi + C_2 \sin m_1 \xi + C_3 \cosh m_2 \xi + C_4 \sinh m_2 \xi \quad (B8)$$

$$\begin{aligned} \bar{\Psi}(\xi, p) = & \frac{1}{m_1} \left[m_1^2 + \left(\frac{c_1}{c_2} \right)^2 p^2 \right] (C_2 \cos m_1 \xi - C_1 \sin m_1 \xi) + \\ & \frac{1}{m_2} \left[m_2^2 - \left(\frac{c_1}{c_2} \right)^2 p^2 \right] (C_4 \cosh m_2 \xi + C_3 \sinh m_2 \xi) \end{aligned} \quad (B9)$$

where C_1 , C_2 , C_3 , and C_4 are functions of p which must be chosen so that the boundary conditions are satisfied.

Specific Problems

Cantilever beam given a step velocity at the root. - If the root $\xi = 0$ of a cantilever beam is given a step velocity $\bar{v} = \frac{c_1}{c_2} \bar{y}_\tau = 1$ at time $\tau = 0$, the boundary conditions may be written

$$\left. \begin{aligned} \bar{y}(0, \tau) &= \frac{c_2}{c_1} \tau \\ \psi(0, \tau) &= 0 \\ \psi_\xi(1, \tau) &= 0 \\ \psi(1, \tau) &= \bar{y}_\xi(1, \tau) \end{aligned} \right\} \quad (B10)$$

These boundary conditions transform to (transform 8, table I)

$$\left. \begin{aligned} Y(0, p) &= \frac{c_2}{c_1} \frac{1}{p^2} \\ \bar{\Psi}(0, p) &= 0 \\ \bar{\Psi}_\xi(1, p) &= 0 \\ \bar{\Psi}(1, p) &= Y_\xi(1, p) \end{aligned} \right\} \quad (B11)$$

The constants C_1 , C_2 , C_3 , and C_4 are determined by substituting equations (B8) and (B9) into equations (B11); the resulting expressions for $Y(\xi, p)$ and $\bar{\Psi}(\xi, p)$ may be written in the forms

$$Y(\xi, p) = \frac{c_2}{c_1} \frac{U_Y(\xi, p)}{p^2 D(p)} \quad (B12)$$

and

$$\Psi(\xi, p) = \frac{c_2}{c_1} \frac{U_\Psi(\xi, p)}{p^2 D(p)} \quad (B13)$$

where

$$\begin{aligned} U_Y(\xi, p) = & \left(1 - \frac{m_1}{m_2} \sin m_1 \sinh m_2 + \frac{1}{Q} \cos m_1 \cosh m_2\right) \cos m_1 \xi + \\ & \left(1 + \frac{m_2}{m_1} \sin m_1 \sinh m_2 + Q \cos m_1 \cosh m_2\right) \cosh m_2 \xi + \\ & \left(\frac{1}{Q} \sin m_1 \cosh m_2 + \frac{m_1}{m_2} \cos m_1 \sinh m_2\right) \sin m_1 \xi - \\ & \left(\frac{m_2}{m_1} \sin m_1 \cosh m_2 + Q \cos m_1 \sinh m_2\right) \sinh m_2 \xi \\ U_\Psi(\xi, p) = & \frac{m_2^2 - \left(\frac{c_1}{c_2}\right)^2 p^2}{m_2} \left[\left(\frac{m_2}{m_1} \sin m_1 \cosh m_2 + Q \cos m_1 \sinh m_2\right) (\cos m_1 \xi - \right. \\ & \left. \cosh m_2 \xi) - Q \frac{m_2}{m_1} \left(1 - \frac{m_1}{m_2} \sin m_1 \sinh m_2 + \frac{1}{Q} \cos m_1 \cosh m_2\right) \sin m_1 \xi + \right. \\ & \left. \left(1 + \frac{m_2}{m_1} \sin m_1 \sinh m_2 + Q \cos m_1 \cosh m_2\right) \sinh m_2 \xi \right] \end{aligned}$$

$$D(p) = 2 + \left(Q + \frac{1}{Q}\right) \cos m_1 \cosh m_2 + \left(\frac{m_2}{m_1} - \frac{m_1}{m_2}\right) \sin m_1 \sinh m_2$$

$$Q = \frac{m_1^2 + \left(\frac{c_1}{c_2}\right)^2 p^2}{m_2^2 - \left(\frac{c_1}{c_2}\right)^2 p^2}$$

The inverse transforms $\bar{Y}(\xi, \tau)$ and $\Psi(\xi, \tau)$ are determined by substitution of $Y(\xi, p)$ and $\bar{\Psi}(\xi, p)$ into the complex inversion integral (ref. 15). The singularities of the resulting integrands $e^{p\tau}Y(\xi, p)$ and $e^{p\tau}\bar{\Psi}(\xi, p)$ must therefore be examined. Although the functions m_1 and m_2 are, in themselves, multiple-valued functions of p with branch

points at $p = 0$, $\pm i\sqrt{R}$, and $\pm \frac{2\sqrt{R} \frac{c_1}{c_2}}{1 - \left(\frac{c_1}{c_2}\right)^2}$, it follows from a considera-

tion of the fundamental theorem of the uniqueness of solutions of ordinary linear differential equations that $Y(\xi, p)$ and $\bar{\Psi}(\xi, p)$ must nevertheless be single-valued. The integrands $e^{p\tau}Y(\xi, p)$ and $e^{p\tau}\bar{\Psi}(\xi, p)$ thus have no singularities other than poles. The inverse transforms $\bar{Y}(\xi, \tau)$ and $\Psi(\xi, \tau)$ will therefore be taken as the sum of the residues at the poles of $e^{p\tau}Y(\xi, p)$ and $e^{p\tau}\bar{\Psi}(\xi, p)$, respectively (see ref. 15).

It can be shown that no singularities occur in the numerator functions $U_Y(\xi, p)$ and $U_{\bar{\Psi}}(\xi, p)$; therefore, all the poles of $Y(\xi, p)$ and $\bar{\Psi}(\xi, p)$ must be introduced by the zeros of the denominator $p^2 D(p)$. Consider first the equation

$$D(p) = 2 + \left(Q + \frac{1}{Q}\right) \cos m_1 \cosh m_2 + \left(\frac{m_2}{m_1} - \frac{m_1}{m_2}\right) \sin m_1 \sinh m_2 = 0 \quad (B14)$$

This equation has an infinite number of roots $p = \pm p_n$, $n = 1, 2, \dots, \infty$, all of which are, in general, simple poles of both $Y(\xi, p)$ and $\bar{\Psi}(\xi, p)$. In addition, $p = 0$ can be shown to be a double pole of $Y(\xi, p)$ but not a pole of $\bar{\Psi}(\xi, p)$.

The sum of the residues of $e^{p\tau}Y(\xi, p)$ at the poles $p = 0$ and $p = \pm p_n$, $n = 1, 2, 3, \dots, \infty$, is

$$\bar{Y}(\xi, \tau) = \frac{c_2}{c_1} \left\{ \tau + \sum_{n=1}^{\infty} \frac{1}{p_n^2} \left[\frac{U_Y(\xi, p_n)}{D'(p_n)} e^{p_n \tau} + \frac{U_Y(\xi, -p_n)}{D'(-p_n)} e^{-p_n \tau} \right] \right\}$$

and, similarly, the sum of the residues of $e^{p\tau}\Psi(\xi, p)$ at $p = \pm p_n$, $n = 1, 2, 3, \dots, \infty$, may be written

$$\psi(\xi, \tau) = \frac{c_2}{c_1} \sum_{n=1}^{\infty} \frac{1}{p_n^2} \left[\frac{U_{\Psi}(\xi, p_n)}{D'(p_n)} e^{p_n \tau} + \frac{U_{\Psi}(\xi, -p_n)}{D'(-p_n)} e^{-p_n \tau} \right]$$

where

$$D'(p) = \frac{d}{dp} [D(p)]$$

$$\begin{aligned} &= \frac{R_p \left(\frac{c_1}{c_2}\right)^2}{m_1 m_2} \left(\frac{1}{m_2^2} - \frac{1}{m_1^2} \right) \sin m_1 \sinh m_2 - \\ &\quad \frac{\frac{2}{p} \left[\frac{(m_1^2 + m_2^2)^2}{R_p^2 \left(\frac{c_1}{c_2}\right)^2} + 4 \right] \cos m_1 \cosh m_2 + \frac{m_2}{p} \left\{ \left(Q + \frac{1}{Q} \right) \left[1 + \right. \right.}{\left. \frac{R_p^2 \left(\frac{c_1}{c_2}\right)^2}{m_2^2 (m_1^2 + m_2^2)} \right] + \frac{m_2^2 - m_1^2}{m_2^2} \left[1 + \frac{R_p^2 \left(\frac{c_1}{c_2}\right)^2}{m_1^2 (m_1^2 + m_2^2)} \right] \right\} \cos m_1 \sinh m_2 -}{\frac{m_1}{p} \left\{ \left(Q + \frac{1}{Q} \right) \left[1 + \frac{R_p^2 \left(\frac{c_1}{c_2}\right)^2}{m_1^2 (m_1^2 + m_2^2)} \right] - \frac{m_2^2 - m_1^2}{m_1^2} \left[1 + \right. \right.}{\left. \frac{R_p^2 \left(\frac{c_1}{c_2}\right)^2}{m_2^2 (m_1^2 + m_2^2)} \right] \right\} \sin m_1 \cosh m_2} \end{aligned}$$

However, it is seen that $U_Y(\xi, p) = U_Y(\xi, -p)$, $U_{\Psi}(\xi, p) = U_{\Psi}(\xi, -p)$, and $D'(p) = -D'(-p)$ so that these equations reduce to

$$\bar{y}(\xi, \tau) = \frac{c_2}{c_1} \left[\tau + 2 \sum_{n=1}^{\infty} \frac{U_Y(\xi, p_n)}{p_n^2 D'(p_n)} \sinh p_n \tau \right] \quad (B15)$$

and

$$\psi(\xi, \tau) = 2 \frac{c_2}{c_1} \sum_{n=1}^{\infty} \frac{U_{\Psi}(\xi, p_n)}{p_n^2 D'(p_n)} \sinh p_n \tau \quad (B16)$$

If, in equation (B14), p is replaced by ik , the result may be written

$$2 + \left[\frac{(\alpha^2 + \beta^2)^2}{Rk^2 \left(\frac{c_1}{c_2}\right)^2} - 2 \right] \cosh \alpha \cos \beta - \left(\frac{\beta}{\alpha} - \frac{\alpha}{\beta} \right) \sinh \alpha \sin \beta = 0 \quad (B17)$$

where

$$\alpha = k \sqrt{\frac{-\left[1 + \left(\frac{c_1}{c_2}\right)^2\right] + \sqrt{\left[1 - \left(\frac{c_1}{c_2}\right)^2\right]^2 + \frac{4R}{k^2} \left(\frac{c_1}{c_2}\right)^2}}{2}}$$

$$\beta = k \sqrt{\frac{1 + \left(\frac{c_1}{c_2}\right)^2 + \sqrt{\left[1 - \left(\frac{c_1}{c_2}\right)^2\right]^2 + \frac{4R}{k^2} \left(\frac{c_1}{c_2}\right)^2}}{2}}$$

and $k = \frac{\Omega L}{c_1}$, Ω being the circular frequency of vibration. Equation (B17) is the frequency equation for a uniform cantilever beam (see ref. 5) and its solutions $k = k_n$, $n = 1, 2, 3, \dots, \infty$, are the non-dimensional natural vibration frequencies of such a beam. Equations (B15) and (B16) may be written in terms of these natural frequencies simply by replacing p_n by ik_n . The results are

$$\bar{y}(\xi, \tau) = \frac{c_2}{c_1} \left[\tau + 2 \sum_{n=1}^{\infty} X_{\bar{y}_n}(\xi) \sin k_n \tau \right] \quad (B18)$$

and

$$\psi(\xi, \tau) = 2 \frac{c_2}{c_1} \sum_{n=1}^{\infty} X_{\psi_n}(\xi) \sin k_n \tau \quad (B19)$$

where

$$\begin{aligned} X_{\bar{y}_n}(\xi) = & \frac{1}{k_n \phi_n} \left[\left(1 + \frac{\alpha_n}{\beta_n} \sin \beta_n \sinh \alpha_n + \frac{1}{\phi_n} \cos \beta_n \cosh \alpha_n \right) \cosh \alpha_n \xi + \right. \\ & \left(1 - \frac{\beta_n}{\alpha_n} \sin \beta_n \sinh \alpha_n + \phi_n \cos \beta_n \cosh \alpha_n \right) \cos \beta_n \xi - \\ & \left(\frac{\alpha_n}{\beta_n} \cosh \alpha_n \sin \beta_n + \frac{1}{\phi_n} \sinh \alpha_n \cos \beta_n \right) \sinh \alpha_n \xi + \\ & \left. \left(\frac{\beta_n}{\alpha_n} \sinh \alpha_n \cos \beta_n + \phi_n \cosh \alpha_n \sin \beta_n \right) \sin \beta_n \xi \right] \\ X_{\psi_n}(\xi) = & \frac{\beta_n^2 - \left(\frac{c_1}{c_2} \right)^2 k_n^2}{k_n \beta_n \phi_n} \left[\left(\frac{\beta_n}{\alpha_n} \sinh \alpha_n \cos \beta_n + \phi_n \cosh \alpha_n \sin \beta_n \right) (\cos \beta_n \xi - \right. \\ & \cosh \alpha_n \xi) + \phi_n \frac{\beta_n}{\alpha_n} \left(1 + \frac{\alpha_n}{\beta_n} \sin \beta_n \sinh \alpha_n + \right. \\ & \left. \frac{1}{\phi_n} \cos \beta_n \cosh \alpha_n \right) \sinh \alpha_n \xi - \left(1 - \frac{\beta_n}{\alpha_n} \sin \beta_n \sinh \alpha_n + \right. \\ & \left. \phi_n \cos \beta_n \cosh \alpha_n \right) \sin \beta_n \xi \left. \right] \end{aligned}$$

$$\begin{aligned}
\phi_n = & \frac{Rk_n^2 \left(\frac{c_1}{c_2}\right)^2}{\alpha_n \beta_n} \left(\frac{1}{\beta_n^2} - \frac{1}{\alpha_n^2} \right) \sin \beta_n \sinh \alpha_n + 2 \left[\frac{(\alpha_n^2 + \beta_n^2)^2}{Rk_n^2 \left(\frac{c_1}{c_2}\right)^2} - 4 \right] \cos \beta_n \cosh \alpha_n \\
& \beta_n \left\{ \left[\frac{(\alpha_n^2 + \beta_n^2)^2}{Rk_n^2 \left(\frac{c_1}{c_2}\right)^2} - 2 \right] \left[1 - \frac{Rk_n^2 \left(\frac{c_1}{c_2}\right)^2}{\beta_n^2 (\alpha_n^2 + \beta_n^2)} \right] + \frac{\beta_n^2 - \alpha_n^2}{\beta_n^2} \left[1 - \right. \right. \\
& \left. \left. \frac{Rk_n^2 \left(\frac{c_1}{c_2}\right)^2}{\alpha_n^2 (\alpha_n^2 + \beta_n^2)} \right] \right\} \cosh \alpha_n \sin \beta_n + \alpha_n \left\{ \left[\frac{(\alpha_n^2 + \beta_n^2)^2}{Rk_n^2 \left(\frac{c_1}{c_2}\right)^2} - 2 \right] \left[1 - \right. \right. \\
& \left. \left. \frac{Rk_n^2 \left(\frac{c_1}{c_2}\right)^2}{\alpha_n^2 (\alpha_n^2 + \beta_n^2)} \right] - \frac{\beta_n^2 - \alpha_n^2}{\alpha_n^2} \left[1 - \frac{Rk_n^2 \left(\frac{c_1}{c_2}\right)^2}{\beta_n^2 (\alpha_n^2 + \beta_n^2)} \right] \right\} \sinh \alpha_n \cos \beta_n \\
\phi_n = & \frac{\alpha_n^2 + \left(\frac{c_1}{c_2}\right)^2 k_n^2}{\beta_n^2 - \left(\frac{c_1}{c_2}\right)^2 k_n^2}
\end{aligned}$$

The coefficients $X_{\bar{y}_n}(\xi)$ and $X_{\psi_n}(\xi)$ are seen to be the natural mode shapes associated with the frequency k_n . As a check on the validity of the Laplace transform procedure these quantities may be shown to satisfy the differential equations (B1) and the boundary conditions (B10).

Substituting $\bar{y}(\xi, \tau)$ and $\psi(\xi, \tau)$ from equations (B18) and (B19) into equations (B2) and (B3) gives, for the moment and shear,

$$\bar{M}(\xi, \tau) = -2 \frac{c_2}{c_1} \sum_{n=1}^{\infty} X_{M_n}(\xi) \sin k_n \tau \quad (B20)$$

where

$$\begin{aligned}
 X_{\bar{M}_n}(\xi) = \frac{\beta_n^2 - \left(\frac{c_1}{c_2}\right)^2 k_n^2}{k_n \phi_n} & \left[\phi_n \left(1 + \frac{\alpha_n}{\beta_n} \sin \beta_n \sinh \alpha_n + \right. \right. \\
 & \left. \frac{1}{\phi_n} \cosh \alpha_n \cos \beta_n \right) \cosh \alpha_n \xi - \left(1 - \frac{\beta_n}{\alpha_n} \sin \beta_n \sinh \alpha_n + \right. \\
 & \left. \phi_n \cosh \alpha_n \cos \beta_n \right) \cos \beta_n \xi - \left(\frac{\beta_n}{\alpha_n} \sinh \alpha_n \cos \beta_n + \right. \\
 & \left. \left. \phi_n \cosh \alpha_n \sin \beta_n \right) \left(\sin \beta_n \xi + \frac{\alpha_n}{\beta_n} \sinh \alpha_n \xi \right) \right]
 \end{aligned}$$

and

$$\bar{V}(\xi, \tau) = -2R \frac{c_1}{c_2} \sum_{n=1}^{\infty} X_{\bar{V}_n}(\xi) \sin k_n \tau \quad (B21)$$

where

$$\begin{aligned}
 X_{\bar{V}_n}(\xi) = \frac{k_n}{\beta_n \phi_n} & \left[\frac{\beta_n}{\alpha_n} \left(1 + \frac{\alpha_n}{\beta_n} \sin \beta_n \sinh \alpha_n + \frac{1}{\phi_n} \cos \beta_n \cosh \alpha_n \right) \sinh \alpha_n \xi + \right. \\
 & \left(1 - \frac{\beta_n}{\alpha_n} \sin \beta_n \sinh \alpha_n + \phi_n \cos \beta_n \cosh \alpha_n \right) \sin \beta_n \xi - \\
 & \left. \left(\frac{\beta_n}{\alpha_n} \sinh \alpha_n \cos \beta_n + \phi_n \cosh \alpha_n \sin \beta_n \right) \left(\cos \beta_n \xi + \frac{1}{\phi_n} \cosh \alpha_n \xi \right) \right]
 \end{aligned}$$

The first eight terms in equations (B20) and (B21) have been used to compute the quantities $\bar{M}(0, \tau)$ and $\bar{V}(0, \tau)$. These results have been plotted in the range $0 \leq \tau \leq 10$ in figures 4(a) and 4(b).

Simply supported beam with an applied step end moment.— If a step moment $\bar{M} = 1$ is applied to the end $\xi = 0$ of a simply supported beam at time $\tau = 0$, the boundary conditions are

$$\left. \begin{aligned} \bar{y}(0, \tau) &= 0 \\ \bar{y}(1, \tau) &= 0 \\ \psi_{\xi}(0, \tau) &= -1 \\ \psi_{\xi}(1, \tau) &= 0 \end{aligned} \right\} \quad (B22)$$

These equations transform to (transform 7, table I)

$$\left. \begin{aligned} Y(0, p) &= 0 \\ Y(1, p) &= 0 \\ \bar{\Psi}_{\xi}(0, p) &= -\frac{1}{p} \\ \bar{\Psi}_{\xi}(1, p) &= 0 \end{aligned} \right\} \quad (B23)$$

If conditions (B23) are used to evaluate the functions C_1 , C_2 , C_3 , and C_4 in equations (B8) and (B9), the quantities $Y(\xi, p)$ and $\bar{\Psi}(\xi, p)$ become

$$Y(\xi, p) = \frac{1}{p(m_1^2 + m_2^2)} (\cos m_1 \xi - \cot m_1 \sin m_1 \xi - \cosh m_2 \xi + \coth m_2 \sinh m_2 \xi) \quad (B24)$$

$$\bar{\Psi}(\xi, p) = -\frac{1}{p(m_1^2 + m_2^2)} \left[\frac{m_1^2 + \left(\frac{c_1}{c_2}\right)^2 p^2}{m_1} (\sin m_1 \xi + \cot m_1 \cos m_1 \xi) + \frac{m_2^2 - \left(\frac{c_1}{c_2}\right)^2 p^2}{m_2} (\sinh m_2 \xi - \coth m_2 \cosh m_2 \xi) \right] \quad (B25)$$

or they may be written in the forms

$$Y(\xi, p) = \frac{N_Y(\xi, p)}{D_Y(p)} \quad (B26)$$

where

$$N_Y(\xi, p) = \sin m_1 \sinh m_2 (\cos m_1 \xi - \cosh m_2 \xi) - \cos m_1 \sinh m_2 \sin m_1 \xi + \\ \sin m_1 \cosh m_2 \sinh m_2 \xi$$

$$D_Y(p) = p(m_1^2 + m_2^2) \sin m_1 \sinh m_2$$

and

$$\Psi(\xi, p) = \frac{N_\Psi(\xi, p)}{D_\Psi(p)} \quad (B27)$$

where

$$N_\Psi(\xi, p) = m_1 \left[m_2^2 - \left(\frac{c_1}{c_2} \right)^2 p^2 \right] \sin m_1 (\cosh m_2 \cosh m_2 \xi - \sinh m_2 \sinh m_2 \xi) - \\ m_2 \left[m_1^2 + \left(\frac{c_1}{c_2} \right)^2 p^2 \right] \sinh m_2 (\cos m_1 \cos m_1 \xi + \sin m_1 \sin m_1 \xi)$$

$$D_\Psi(p) = m_1 m_2 D_Y(p)$$

Here again, the functions $Y(\xi, p)$ and $\Psi(\xi, p)$ are single-valued, and the inverse transforms $\bar{y}(\xi, \tau)$ and $\psi(\xi, \tau)$ of the quantities $Y(\xi, p)$ and $\Psi(\xi, p)$ are taken as the sums of the residues at the poles of $e^{p\tau} Y(\xi, p)$ and $e^{p\tau} \Psi(\xi, p)$, respectively. Consider all the roots of the denominators $D_Y(p)$ and $D_\Psi(p)$. For $m_1 = \pm n\pi$ or $m_2 = \pm in\pi$,

$n = 1, 2, 3, \dots \infty$ (any of which are roots of both denominators), equation (B6) becomes

$$p^4 + \left\{ R + n^2 \pi^2 \left[1 + \left(\frac{c_2}{c_1} \right)^2 \right] \right\} p^2 + \left(\frac{c_2}{c_1} \right)^2 n^4 \pi^4 = 0$$

$$(n = 1, 2, 3, \dots \infty) \quad (B28)$$

The solutions of equation (B28) are $p = \pm ia_n$ and $\pm ib_n$, $n = 1, 2, 3, \dots \infty$, where

$$a_n = \sqrt{\frac{R + n^2 \pi^2 \left[1 + \left(\frac{c_2}{c_1} \right)^2 \right] - \sqrt{\left\{ R + n^2 \pi^2 \left[1 + \left(\frac{c_2}{c_1} \right)^2 \right] \right\}^2 - 4 \left(\frac{c_2}{c_1} \right)^2 n^4 \pi^4}}{2}}$$

$$b_n = \sqrt{\frac{R + n^2 \pi^2 \left[1 + \left(\frac{c_2}{c_1} \right)^2 \right] + \sqrt{\left\{ R + n^2 \pi^2 \left[1 + \left(\frac{c_2}{c_1} \right)^2 \right] \right\}^2 - 4 \left(\frac{c_2}{c_1} \right)^2 n^4 \pi^4}}{2}}$$

and these points are seen to be the locations of simple poles of both $Y(\xi, p)$ and $\Psi(\xi, p)$. The roots $p = \pm \frac{2\sqrt{R} \frac{c_2}{c_1}}{1 - \left(\frac{c_2}{c_1} \right)^2}$ of the equation

$m_1^2 + m_2^2 = 0$ are zeros of the denominator, but these are also roots of the numerators $N_Y(\xi, p)$ and $N_\Psi(\xi, p)$ and are not poles of either $Y(\xi, p)$ or $\Psi(\xi, p)$. The root $p = 0$, on the other hand, is a pole of both $Y(\xi, p)$ and $\Psi(\xi, p)$ for, although both numerators also go to zero at this point, the denominators vanish more rapidly. The equation $m_1 = 0$ has three roots: $p = 0$, which has already been discussed, and $p = \pm i\sqrt{R}$. The latter points are not poles of $Y(\xi, p)$ since they are roots of $N_Y(\xi, p) = 0$, but they are simple poles of $\Psi(\xi, p)$.

First consider the residues of $e^{pT} Y(\xi, p)$ and $e^{pT} \Psi(\xi, p)$ at the poles $\pm ia_n$ and $\pm ib_n$. The sums of the residues at these poles provide the results

$$\bar{y}_d(\xi, \tau) = \sum_{n=1}^{\infty} \left[\frac{N_Y(\xi, ia_n)}{D_Y'(ia_n)} e^{ia_n \tau} + \frac{N_Y(\xi, -ia_n)}{D_Y'(-ia_n)} e^{-ia_n \tau} + \frac{N_Y(\xi, ib_n)}{D_Y'(ib_n)} e^{ib_n \tau} + \frac{N_Y(\xi, -ib_n)}{D_Y'(-ib_n)} e^{-ib_n \tau} \right] \quad (B29)$$

and

$$\bar{\psi}_d(\xi, \tau) = \sum_{n=1}^{\infty} \left[\frac{N_{\bar{\psi}}(\xi, ia_n)}{D_{\bar{\psi}}'(ia_n)} e^{ia_n \tau} + \frac{N_{\bar{\psi}}(\xi, -ia_n)}{D_{\bar{\psi}}'(-ia_n)} e^{-ia_n \tau} + \frac{N_{\bar{\psi}}(\xi, ib_n)}{D_{\bar{\psi}}'(ib_n)} e^{ib_n \tau} + \frac{N_{\bar{\psi}}(\xi, -ib_n)}{D_{\bar{\psi}}'(-ib_n)} e^{-ib_n \tau} \right] \quad (B30)$$

where the subscripts on \bar{y} and $\bar{\psi}$ indicate that they constitute only parts - so-called "dynamic" parts - of the complete solutions for $\bar{y}(\xi, \tau)$ and $\bar{\psi}(\xi, \tau)$. In order to obtain the values of $\frac{N_Y}{D_Y'}$ and $\frac{N_{\bar{\psi}}}{D_{\bar{\psi}}'}$ at $p = \pm ia_n$ and $\pm ib_n$, it is necessary to use the fact that, when p equals one of the roots $\pm ia_n$ and $\pm ib_n$, one of four equations $m_1 = n\pi$, $m_1 = -n\pi$, $m_2 = n\pi$, or $m_2 = -n\pi$ is satisfied. The question of which value of p corresponds to each equation need not be answered since the following relationships can be derived:

$$\left(\frac{N_Y}{D_Y'} \right)_{m_1=n\pi} = \left(\frac{N_Y}{D_Y'} \right)_{m_1=-n\pi} = \left(\frac{N_Y}{D_Y'} \right)_{m_2=n\pi} = \left(\frac{N_Y}{D_Y'} \right)_{m_2=-n\pi} = - \frac{\left(\frac{c_2}{c_1} \right)^2 n\pi \sin n\pi \xi}{2a_n^2 b_n^2 + p^2 (a_n^2 + b_n^2)} \quad (B31)$$

$$\left(\frac{N_{\bar{\psi}}}{D_{\bar{\psi}}'} \right)_{m_1=n\pi} = \left(\frac{N_{\bar{\psi}}}{D_{\bar{\psi}}'} \right)_{m_1=-n\pi} = \left(\frac{N_{\bar{\psi}}}{D_{\bar{\psi}}'} \right)_{m_2=n\pi} = \left(\frac{N_{\bar{\psi}}}{D_{\bar{\psi}}'} \right)_{m_2=-n\pi} = - \frac{\left(\frac{c_2}{c_1} \right)^2 \left[n^2 \pi^2 + \left(\frac{c_1}{c_2} \right)^2 p^2 \right] \cos n\pi \xi}{2a_n^2 b_n^2 + p^2 (a_n^2 + b_n^2)} \quad (B32)$$

As an example, let $p = ia_n$. Then one of the four possibilities $m_1 = n\pi$, $m_1 = -n\pi$, $m_2 = in\pi$, and $m_2 = -in\pi$ must occur. But for any of these possibilities, the ratios $\frac{N_Y}{D_Y'}$ and $\frac{N_\Psi}{D_\Psi'}$ have the forms given by equations (B31) and (B32). Thus,

$$\left. \begin{aligned} \frac{N_Y(\xi, ia_n)}{D_Y'(ia_n)} &= \frac{\left(\frac{c_2}{c_1}\right)^2 n\pi \sin n\pi\xi}{a_n^2(a_n^2 - b_n^2)} \\ \frac{N_\Psi(\xi, ia_n)}{D_\Psi'(ia_n)} &= \frac{\left[\left(\frac{c_2}{c_1}\right)^2 \frac{n^2\pi^2}{a_n^2} - 1\right] \cos n\pi\xi}{a_n^2 - b_n^2} \end{aligned} \right\} \quad (B33)$$

The values of the other necessary ratios can be found in a similar manner and equations (B29) and (B30) reduce to

$$\bar{y}_d(\xi, \tau) = 2\left(\frac{c_2}{c_1}\right)^2 \sum_{n=1}^{\infty} \frac{n\pi \sin n\pi\xi}{a_n^2 - b_n^2} \left(\frac{\cos a_n\tau}{a_n^2} - \frac{\cos b_n\tau}{b_n^2} \right) \quad (B34)$$

and

$$\psi_{d1}(\xi, \tau) = 2 \sum_{n=1}^{\infty} \frac{\cos n\pi\xi}{a_n^2 - b_n^2} \left[\left(\frac{b_n^2}{n^2\pi^2} - 1 \right) \cos a_n\tau - \left(\frac{a_n^2}{n^2\pi^2} - 1 \right) \cos b_n\tau \right] \quad (B35)$$

Next, consider the contributions of the pole at $p = 0$. Equations (B24) and (B25) may be expanded in a Laurent series about $p = 0$. The resulting equations for $Y(\xi, p)$ and $\Psi(\xi, p)$ may be written

$$Y(\xi, p) = \frac{1}{p} \left[\frac{\xi^3}{6} - \frac{\xi^2}{2} + \frac{\xi}{3} + O(p) \right] \quad (B36)$$

$$\Psi(\xi, p) = \frac{1}{p} \left[\frac{\xi^2}{2} - \xi + \frac{1}{3} + \frac{1}{R} + O(p) \right] \quad (B37)$$

where $O(p)$ signifies terms of order p or higher. Thus the quantities $e^{p\tau}Y(\xi, p)$ and $e^{p\tau}\bar{Y}(\xi, p)$ have simple poles at $p = 0$ with the residues

$$\bar{y}_{st}(\xi, \tau) = \frac{\xi^3}{6} - \frac{\xi^2}{2} + \frac{\xi}{3} \quad (B38)$$

and

$$\psi_{st}(\xi, \tau) = \frac{\xi^2}{2} - \xi + \frac{1}{3} + \frac{1}{R} \quad (B39)$$

respectively. It can be readily verified that equations (B38) and (B39) actually constitute the solution of the problem when the beam is considered to be loaded statically.

Lastly, consider the points $p = \pm i\sqrt{R}$, which are simple poles of $\bar{Y}(\xi, p)$. It can be shown that

$$\lim_{p \rightarrow \pm i\sqrt{R}} \frac{N\bar{Y}}{D\bar{Y}} = -\frac{1}{2R} \quad (B40)$$

so that the sum of the residues of $e^{p\tau}\bar{Y}(\xi, p)$ at these poles provides the additional dynamic contribution

$$\psi_{d2}(\xi, \tau) = -\frac{1}{R} \cos \sqrt{R} \tau \quad (B41)$$

Summing the contributions of all the poles gives

$$\bar{y}(\xi, \tau) = \frac{\xi^3}{6} - \frac{\xi^2}{2} + \frac{\xi}{3} + 2\left(\frac{c_2}{c_1}\right)^2 \sum_{n=1}^{\infty} \frac{n\pi \sin n\pi\xi}{a_n^2 - b_n^2} \left(\frac{\cos a_n\tau}{a_n^2} - \frac{\cos b_n\tau}{b_n^2} \right) \quad (B42)$$

$$\psi(\xi, \tau) = \frac{\xi^2}{2} - \xi + \frac{1}{3} + \frac{1}{R} - \frac{1}{R} \cos \sqrt{R} \tau + 2 \sum_{n=1}^{\infty} \frac{\cos n\pi\xi}{a_n^2 - b_n^2} \left[\left(\frac{b_n^2}{n^2\pi^2} - 1 \right) \cos a_n\tau - \right.$$

$$\left. \left(\frac{a_n^2}{n^2\pi^2} - 1 \right) \cos b_n\tau \right] \quad (B43)$$

The responses $\bar{y}(\xi, \tau)$ and $\psi(\xi, \tau)$ are seen to have the same form as solutions obtained by Williams' method (ref. 2); that is, they are the sum of a static part, $\bar{y}_{st}(\xi, \tau)$ and $\psi_{st}(\xi, \tau)$, and a dynamic correction, $\bar{y}_d(\xi, \tau)$ and $\psi_{d1}(\xi, \tau) + \psi_{d2}(\xi, \tau)$, which is expanded in a series of the natural mode shapes. The \bar{y} - and ψ -components of the natural modes have the shapes $\sin n\pi\xi$ and $\cos n\pi\xi$, respectively, and there are seen to be two natural frequencies, a_n and b_n , associated with each integer n so that each integer corresponds to two modes. From equations (B2) and (B3),

$$\bar{M}(\xi, \tau) = 1 - \xi + 2 \sum_{n=1}^{\infty} \frac{n\pi \sin n\pi\xi}{a_n^2 - b_n^2} \left[\left(\frac{b_n^2}{n^2\pi^2} - 1 \right) \cos a_n\tau - \left(\frac{a_n^2}{n^2\pi^2} - 1 \right) \cos b_n\tau \right] \quad (B44)$$

and

$$\bar{V}(\xi, \tau) = \cos \sqrt{R} \tau - 1 + 2R \sum_{n=1}^{\infty} \frac{\cos n\pi\xi}{a_n^2 - b_n^2} (\cos a_n\tau - \cos b_n\tau) \quad (B45)$$

Six terms ($n = 3$) have been used in the summations of equations (B44) and (B45) in computing the quantities $\bar{M}(1/2, \tau)$ and $\bar{V}(0, \tau)$. These results have been plotted in figures 5(a) and 5(b) up to $\tau = 8$.

Simply supported beam with an applied ramp-platform end moment. - Let the response to unit step moment at $\xi = 0$, obtained above, be designated $\bar{M}_1(\xi, \tau)$ and $\bar{V}_1(\xi, \tau)$. Then the response to an arbitrary applied moment $\bar{M}(0, \tau)$ may be obtained from Duhamel's superposition integral as

$$\left. \begin{aligned} \bar{M}(\xi, \tau) &= \bar{M}(0, 0)\bar{M}_1(\xi, \tau) + \int_0^\tau \bar{M}_1(\xi, \tau-\theta)\bar{M}_\theta(0, \theta)d\theta \\ \bar{V}(\xi, \tau) &= \bar{M}(0, 0)\bar{V}_1(\xi, \tau) + \int_0^\tau \bar{V}_1(\xi, \tau-\theta)\bar{M}_\theta(0, \theta)d\theta \end{aligned} \right\} \quad (B46)$$

where the subscript θ indicates differentiation with respect to that variable. Let the applied moment have the ramp-platform time history

$$\left. \begin{aligned} \bar{M}(0, \tau) &= \tau & (0 \leq \tau \leq 1) \\ \bar{M}(0, \tau) &= 1 & (\tau > 1) \end{aligned} \right\} \quad (B47)$$

Then equations (B46) become

$$\left. \begin{aligned} \bar{M}(\xi, \tau) &= \int_0^\tau \bar{M}_1(\xi, \tau - \theta) d\theta & (0 \leq \tau \leq 1) \\ \bar{M}(\xi, \tau) &= \int_0^1 \bar{M}_1(\xi, \tau - \theta) d\theta & (\tau > 1) \end{aligned} \right\} \quad (B48)$$

and

$$\left. \begin{aligned} \bar{V}(\xi, \tau) &= \int_0^\tau \bar{V}_1(\xi, \tau - \theta) d\theta & (0 \leq \tau \leq 1) \\ \bar{V}(\xi, \tau) &= \int_0^1 \bar{V}_1(\xi, \tau - \theta) d\theta & (\tau > 1) \end{aligned} \right\} \quad (B49)$$

Substituting \bar{M}_1 and \bar{V}_1 from equations (B44) and (B45) gives for \bar{M} and \bar{V}

$$\left. \begin{aligned} \bar{M}(\xi, \tau) &= (1 - \xi)\tau + 2 \sum_{n=1}^{\infty} \frac{n\pi \sin n\pi\xi}{a_n^2 - b_n^2} \left[\left(\frac{b_n^2}{n^2\pi^2} - 1 \right) \frac{\sin a_n\tau}{a_n} - \right. \\ &\quad \left. \left(\frac{a_n^2}{n^2\pi^2} - 1 \right) \frac{\sin b_n\tau}{b_n} \right] & (0 \leq \tau \leq 1) \\ \bar{M}(\xi, \tau) &= 1 - \xi + 2 \sum_{n=1}^{\infty} \frac{n\pi \sin n\pi\xi}{a_n^2 - b_n^2} \left[\left(\frac{b_n^2}{n^2\pi^2} - 1 \right) \frac{\sin a_n\tau - \sin a_n(\tau - 1)}{a_n} - \right. \\ &\quad \left. \left(\frac{a_n^2}{n^2\pi^2} - 1 \right) \frac{\sin b_n\tau - \sin b_n(\tau - 1)}{b_n} \right] & (\tau > 1) \end{aligned} \right\} \quad (B50)$$

and

$$\left. \begin{aligned}
 \bar{V}(\xi, \tau) &= \frac{1}{\sqrt{R}} \sin \sqrt{R} \tau - \tau + 2R \sum_{n=1}^{\infty} \frac{\cos n\pi\xi}{a_n^2 - b_n^2} \left(\frac{\sin a_n \tau}{a_n} - \frac{\sin b_n \tau}{b_n} \right) \\
 &\hspace{15em} (0 \leq \tau \leq 1) \\
 \bar{V}(\xi, \tau) &= \frac{1}{\sqrt{R}} \left[\sin \sqrt{R} \tau - \sin \sqrt{R}(\tau - 1) \right] - 1 + \\
 &\quad 2R \sum_{n=1}^{\infty} \frac{\cos n\pi\xi}{a_n^2 - b_n^2} \left[\frac{\sin a_n \tau - \sin a_n(\tau - 1)}{a_n} - \right. \\
 &\quad \left. \frac{\sin b_n \tau - \sin b_n(\tau - 1)}{b_n} \right] \\
 &\hspace{15em} (\tau > 1)
 \end{aligned} \right\} \quad (B51)$$

As in the preceding case, computations using terms up to $n = 3$ in equations (B50) and (B51) have been made for $\bar{M}(1/2, \tau)$ and $\bar{V}(0, \tau)$ in the range $0 \leq \tau \leq 8$. The results are plotted in figures 6(a) and 6(b).

APPENDIX C

EXACT CLOSED SOLUTIONS FOR UNIFORM BEAMS WITH $c_1 = c_2$

Introduction

In this appendix some exact closed solutions of Timoshenko's equations are derived for infinitely long uniform beams for which $c_1 = c_2$. The results for beams of infinite length are then utilized to obtain results for beams of finite length. This is done either by simply restricting the infinite-beam solution to a time interval in which it coincides with the corresponding finite-beam solution or by superposing infinite-beam solutions in such a way that the result satisfies the boundary conditions for a finite beam.

Equations

If the propagation velocities c_1 and c_2 are taken to be equal and if $\bar{q} = 0$, equations (14) reduce to

$$\bar{\omega}_\xi + \bar{M}_\tau = 0 \quad (\text{C1a})$$

$$\bar{V}_\xi - 4\lambda^2 \bar{V}_\tau = 0 \quad (\text{C1b})$$

$$\bar{M}_\xi + \bar{\omega}_\tau - \bar{V} = 0 \quad (\text{C1c})$$

$$\bar{V}_\xi - \frac{1}{4\lambda^2} \bar{V}_\tau - \bar{\omega} = 0 \quad (\text{C1d})$$

where $\lambda = \frac{L}{2r_1}$. This system may be further reduced by writing a linear combination of equations (C1a) and (C1b) and a linear combination of (C1c) and (C1d) to obtain

$$Z_\xi + 2\lambda i K_\tau = 0 \quad (\text{C2a})$$

$$Z_\tau + 2\lambda i K_\xi - 2\lambda i Z = 0 \quad (\text{C2b})$$

in terms of the complex variables $Z = \bar{V} + 2\lambda i \bar{\omega}$ and $K = \bar{M} + 2\lambda i \bar{V}$.

For a beam initially at rest, equations (C2) may be transformed to (transform 6, table I)

$$\xi_{\xi} + 2\lambda i p \kappa = 0 \quad (C3a)$$

$$2\lambda i \kappa_{\xi} + (p - 2\lambda i) \xi = 0 \quad (C3b)$$

in terms of the Laplace transforms $\xi(\xi, p) = \int_0^{\infty} e^{-p\tau} Z(\xi, \tau) d\tau$ and $\kappa(\xi, p) = \int_0^{\infty} e^{-p\tau} K(\xi, \tau) d\tau$. Eliminating κ produces the equation

$$\xi_{\xi\xi} - p(p - 2\lambda i) \xi = 0$$

which has the solution

$$\xi(\xi, p) = A(p) e^{-\xi \sqrt{p(p-2\lambda i)}} + B(p) e^{\xi \sqrt{p(p-2\lambda i)}} \quad (C4)$$

where A and B are governed by the boundary conditions. If the beam extends to infinity in the positive ξ -direction, boundary conditions stipulating that the beam remain undisturbed at $\xi = \infty$ must be satisfied. Thus, equation (C4) reduces to

$$\xi(\xi, p) = A(p) e^{-\xi \sqrt{p(p-2\lambda i)}} \quad (C5)$$

Substituting this expression into equation (C3a) produces

$$\kappa(\xi, p) = \frac{A(p)}{2\lambda i p} \sqrt{p(p - 2\lambda i)} e^{-\xi \sqrt{p(p-2\lambda i)}} \quad (C6)$$

The quantity $A(p)$ may now be determined from the remaining boundary conditions in conjunction with equation (C5) or (C6), or both.

Specific Problems

Infinite cantilever given a step velocity at the root.- If the end $\xi = 0$ of an infinitely long beam is restrained from rotating and

is given a unit step velocity at time $\tau = 0$, the boundary conditions are $\bar{v}(0, \tau) = 1$ and $\bar{\omega}(0, \tau) = 0$. In terms of Z and K these conditions may be written

$$\text{I.P.} [\bar{Z}(0, \tau)] = 0$$

and

$$\text{I.P.} [\bar{K}(0, \tau)] = 2\lambda$$

where I.P. designates the imaginary part of the quantity in brackets. The boundary conditions may be transformed to (transform 7, table I)

$$\text{I.P.} [\bar{\xi}(0, p)] = 0 \quad (\text{C7a})$$

and

$$\text{I.P.} [\bar{\kappa}(0, p)] = \frac{2\lambda}{p} \quad (\text{C7b})$$

respectively.

Because of the nature of these conditions, it will be convenient to proceed in the following manner to determine the function $A(p)$. From equation (C5), it may be seen that $A(p) = \xi(0, p)$; thus condition (C7a) establishes at once that $A(p)$ for this problem is a real quantity. At $\xi = 0$ equation (C6) becomes

$$\kappa(0, p) = \frac{A(p)}{2\lambda ip} \sqrt{p(p - 2\lambda i)}$$

or, in view of condition (C7b),

$$\text{R.P.} [\bar{\kappa}(0, p)] + \frac{2\lambda i}{p} = \frac{A(p)}{2\lambda ip} \sqrt{p(p - 2\lambda i)} \quad (\text{C8})$$

where $\text{R.P.} [\bar{\kappa}(0, p)]$ is the real part of $\bar{\kappa}(0, p)$. Since $A(p)$ and p are real, the conjugate equation, which must also hold, is

$$\text{R.P.} [\bar{\kappa}(0, p)] - \frac{2\lambda i}{p} = -\frac{A(p)}{2\lambda ip} \sqrt{p(p + 2\lambda i)} \quad (\text{C9})$$

Eliminating R.P. $[k(0,p)]$ between equations (C8) and (C9) results in

$$A(p) = -2\lambda i \left(\sqrt{\frac{p - 2\lambda i}{p}} - \sqrt{\frac{p + 2\lambda i}{p}} \right) \quad (C10)$$

If $A(p)$ is substituted into equation (C5), the result may be written in the form

$$\zeta(\xi, p) = - \left[4\lambda^2 + 2\lambda i (p - \sqrt{p^2 + 4\lambda^2}) \right] \frac{e^{-\xi \sqrt{p(p-2\lambda i)}}}{\sqrt{p(p-2\lambda i)}}$$

which has the inverse transform (transforms 1, 3, 14, and 15, table I)

$$Z(\xi, \tau) = -4\lambda^2 \left\{ e^{i\lambda\tau} J_0(\lambda \sqrt{\tau^2 - \xi^2}) - \int_{\xi}^{\tau} e^{i\lambda\theta} J_0(\lambda \sqrt{\theta^2 - \xi^2}) \frac{J_1[2\lambda(\tau - \theta)]}{\tau - \theta} d\theta \right\} \quad (\tau > \xi) \quad (C11)$$

where J_0 and J_1 are Bessel functions of the first kind. From equation (C11) the shear and angular velocity are obtained as

$$\bar{V}(\xi, \tau) = -4\lambda^2 \left\{ \cos \lambda\tau J_0(\lambda \sqrt{\tau^2 - \xi^2}) + \int_{\xi}^{\tau} \sin \lambda\theta J_0(\lambda \sqrt{\theta^2 - \xi^2}) \frac{J_1[2\lambda(\tau - \theta)]}{\tau - \theta} d\theta \right\} \quad (\tau > \xi) \quad (C12)$$

and

$$\bar{\omega}(\xi, \tau) = -2\lambda \left\{ \sin \lambda\tau J_0(\lambda \sqrt{\tau^2 - \xi^2}) - \int_{\xi}^{\tau} \cos \lambda\theta J_0(\lambda \sqrt{\theta^2 - \xi^2}) \frac{J_1[2\lambda(\tau - \theta)]}{\tau - \theta} d\theta \right\} \quad (\tau > \xi) \quad (C13)$$

in terms of integrals that apparently defy evaluation by analytical methods.

The time history of the shear $\bar{V}(0, \tau)$ at the root of the beam may be obtained as a special case of equation (C12); however, it will be noted that $L\{\bar{V}(0, \tau)\} = \xi(0, p) = A(p)$ (where $L\{\bar{V}(0, \tau)\}$ denotes the Laplace transform of $\bar{V}(0, \tau)$) so that the inverse of equation (C10) gives $\bar{V}(0, \tau)$ directly. Thus the shear at the root is found explicitly in terms of tabulated functions as (transform 13, table I)

$$\bar{V}(0, \tau) = -4\lambda^2 [\cos \lambda \tau J_0(\lambda \tau) + \sin \lambda \tau J_1(\lambda \tau)] \quad (\tau > 0) \quad (C14)$$

Since $A(p)$ may be replaced by $L\{\bar{V}(0, \tau)\}$, the inverse transform of equation (C6) may be written for this problem in the form (transforms 1, 2, 3, and 17, table I)

$$K(\xi, \tau) = -\frac{1}{2} \left\{ \frac{1}{\lambda} e^{i\lambda \xi} \bar{V}(0, \tau - \xi) - \int_{\xi}^{\tau} \bar{V}(0, \tau - \theta) e^{i\lambda \theta} \left[\frac{\theta J_1(\lambda \sqrt{\theta^2 - \xi^2})}{\sqrt{\theta^2 - \xi^2}} + iJ_0(\lambda \sqrt{\theta^2 - \xi^2}) \right] d\theta \right\} \quad (\tau > \xi)$$

or, after integration by parts,

$$K(\xi, \tau) = 2\lambda i e^{i\lambda \tau} J_0(\lambda \sqrt{\tau^2 - \xi^2}) - \int_{\xi}^{\tau} \left\{ \bar{V}(0, \tau - \theta) + \frac{2\lambda i}{\tau - \theta} \sin \lambda(\tau - \theta) J_1[\lambda(\tau - \theta)] \right\} e^{i\lambda \theta} J_0(\lambda \sqrt{\theta^2 - \xi^2}) d\theta \quad (\tau > \xi) \quad (C15)$$

where $\bar{V}(0, \tau)$ is defined by equation (C14). From equation (C15) the moment and linear velocity may be written as

$$\bar{M}(\xi, \tau) = -2\lambda \sin \lambda \tau J_0(\lambda \sqrt{\tau^2 - \xi^2}) - 2\lambda \int_{\xi}^{\tau} \left\{ \frac{1}{2\lambda} \bar{V}(0, \tau - \theta) \cos \lambda \theta - \frac{\sin \lambda \theta}{\tau - \theta} \sin \lambda(\tau - \theta) J_1[\lambda(\tau - \theta)] \right\} J_0(\lambda \sqrt{\theta^2 - \xi^2}) d\theta \quad (\tau > \xi) \quad (C16)$$

and

$$\bar{v}(\xi, \tau) = \cos \lambda \tau J_0(\lambda \sqrt{\tau^2 - \xi^2}) - \int_{\xi}^{\tau} \left\{ \frac{1}{2\lambda} \bar{v}(0, \tau - \theta) \sin \lambda \theta + \frac{\cos \lambda \theta}{\tau - \theta} \sin \lambda(\tau - \theta) J_1[\lambda(\tau - \theta)] \right\} J_0(\lambda \sqrt{\theta^2 - \xi^2}) d\theta \quad (\tau > \xi) \quad (C17)$$

again in terms of integrals requiring evaluation by approximate methods.

As in the case of the shear, it will be more convenient to determine the moment $\bar{M}(0, \tau)$ at the root by means other than a reduction of the general relation, equation (C16). Since, for this problem, R.P. $[\kappa(0, p)] = L\{\bar{M}(0, \tau)\}$, equation (C8) may be written, after substitution for $A(p)$, in the form

$$L\{\bar{M}(0, \tau)\} = \frac{1}{p} (\sqrt{p^2 + 4\lambda^2} - p)$$

The inverse transform of this equation is (transforms 4 and 14, table I)

$$\bar{M}(0, \tau) = 2\lambda \int_0^{\tau} \frac{J_1(2\lambda\theta)}{\theta} d\theta \quad (\tau > 0) \quad (C18)$$

But, from reference 17,

$$\frac{J_1(2\lambda\tau)}{\tau} = 2\lambda J_0(2\lambda\tau) - \frac{d}{d\tau} [J_1(2\lambda\tau)]$$

and

$$\int_0^{\tau} J_0(2\lambda\theta) d\theta = \tau \left\{ J_0(2\lambda\tau) + \frac{\pi}{2} [J_1(2\lambda\tau) H_0(2\lambda\tau) - J_0(2\lambda\tau) H_1(2\lambda\tau)] \right\}$$

where H_0 and H_1 are Struve functions. Thus, equation (C18) becomes

$$\bar{M}(0, \tau) = 2\lambda \left\{ \lambda \tau [2 - \pi H_1(2\lambda\tau)] J_0(2\lambda\tau) - [1 - \pi \lambda \tau H_0(2\lambda\tau)] J_1(2\lambda\tau) \right\} \quad (\tau > 0) \quad (C19)$$

The Struve functions H_0 and H_1 are tabulated in reference 17 in the range $0 \leq 2\lambda\tau \leq 15.9$. For larger values of the argument, it is convenient to use the approximations (ref. 17)

$$H_0(2\lambda\tau) \approx Y_0(2\lambda\tau) + \frac{1}{\pi\lambda\tau} \quad (2\lambda\tau > 15.9)$$

$$H_1(2\lambda\tau) \approx Y_1(2\lambda\tau) + \frac{2}{\pi} \left(1 + \frac{1}{4\lambda^2\tau^2} \right) \quad (2\lambda\tau > 15.9)$$

where Y_0 and Y_1 are Bessel functions of the second kind. From reference 18,

$$Y_0(2\lambda\tau)J_1(2\lambda\tau) - Y_1(2\lambda\tau)J_0(2\lambda\tau) = \frac{1}{\pi\lambda\tau}$$

so that

$$\bar{M}(0,\tau) \approx 2\lambda \left[1 - \frac{J_0(2\lambda\tau)}{2\lambda\tau} \right] \quad (2\lambda\tau > 15.9) \quad (C20)$$

Computed values of $\bar{V}(0,\tau)$ and $\bar{M}(0,\tau)$, obtained from equations (C14), (C19), and (C20) for a beam with $\lambda = 5$, have been plotted in figures 4(a) and 4(b), respectively, in the range $0 \leq \tau \leq 2$. In this range, the root of a finite cantilever beam behaves as if the beam were infinite, since the effect of the free end is not felt until the return of the wave front at $\tau = 2$.

Infinite simply supported beam with an applied step end moment.- If the end $\xi = 0$ of an infinitely long beam is simply supported and is subjected to a unit step bending moment at time $\tau = 0$, the boundary conditions are $\bar{M}(0,\tau) = 1$ and $\bar{V}(0,\tau) = 0$, or $K(0,\tau) = 1$. This condition transforms to (transform 7, table I)

$$\kappa(0,p) = \frac{1}{p} \quad (C21)$$

Substituting equation (C6) into condition (C21) reveals that

$$A(p) = \frac{2\lambda i}{\sqrt{p(p - 2\lambda i)}} \quad (C22)$$

so that equations (C5) and (C6) become

$$\xi(\xi, p) = 2\lambda i \frac{e^{-\xi\sqrt{p(p-2\lambda i)}}}{\sqrt{p(p-2\lambda i)}} \quad (C23)$$

and

$$\kappa(\xi, p) = \frac{1}{p} e^{-\xi\sqrt{p(p-2\lambda i)}} \quad (C24)$$

respectively. The inverse transform of equation (C23) is (transforms 3 and 15, table I)

$$Z(\xi, \tau) = 2\lambda i e^{i\lambda\tau} J_0(\lambda\sqrt{\tau^2 - \xi^2}) \quad (\tau > \xi) \quad (C25)$$

and the inverse of equation (C24) may be written (transforms 2, 3, 4, and 16, table I) as

$$K(\xi, \tau) = e^{i\lambda\xi} - \lambda\xi \int_{\xi}^{\tau} e^{i\lambda\theta} \frac{J_1(\lambda\sqrt{\theta^2 - \xi^2})}{\sqrt{\theta^2 - \xi^2}} d\theta \quad (\tau > \xi) \quad (C26)$$

From these equations, the shear, angular velocity, moment, and linear velocity are obtained as

$$\bar{V}(\xi, \tau) = -2\lambda \sin \lambda\tau J_0(\lambda\sqrt{\tau^2 - \xi^2}) \quad (\tau > \xi) \quad (C27)$$

$$\bar{\omega}(\xi, \tau) = \cos \lambda\tau J_0(\lambda\sqrt{\tau^2 - \xi^2}) \quad (\tau > \xi) \quad (C28)$$

$$\bar{M}(\xi, \tau) = \cos \lambda\xi - \lambda\xi \int_{\xi}^{\tau} \cos \lambda\theta \frac{J_1(\lambda\sqrt{\theta^2 - \xi^2})}{\sqrt{\theta^2 - \xi^2}} d\theta \quad (\tau > \xi) \quad (C29)$$

$$\bar{v}(\xi, \tau) = \sin \lambda\xi - \lambda\xi \int_{\xi}^{\tau} \sin \lambda\theta \frac{J_1(\lambda\sqrt{\theta^2 - \xi^2})}{\sqrt{\theta^2 - \xi^2}} d\theta \quad (\tau > \xi) \quad (C30)$$

Thus, \bar{V} and $\bar{\omega}$ are determined everywhere in closed form in terms of tabulated functions, but the relations for \bar{M} and \bar{v} contain integrals which must be evaluated by approximate methods.

The results of this section are utilized in the next where a finite simply supported beam is considered.

Finite simply supported beam with an applied step end moment.- If the end $\xi = 0$ of a finite simply supported beam is subjected to a unit step bending moment at time $\tau = 0$, the boundary conditions may be written

$$\left. \begin{aligned} \bar{M}(0, \tau) &= 1 \\ \bar{v}(0, \tau) &= \bar{M}(1, \tau) = \bar{v}(1, \tau) = 0 \end{aligned} \right\} \quad (C31)$$

or, in terms of K ,

$$\left. \begin{aligned} K(0, \tau) &= 1 \\ K(1, \tau) &= 0 \end{aligned} \right\} \quad (C32)$$

Although a direct solution of equations (C2) is possible in this case, the response of the finite beam may be obtained by a somewhat simpler procedure in which the responses of infinite beams to the same disturbance are superposed. This procedure is described below.

A series of semi-infinite simply supported uniform beams extending in opposite directions are shown in figure 7. The beams have been positioned in the figure so that the origins of the space coordinate ξ lie on the same vertical line, and the segments of greatest interest, $0 \leq \xi \leq 1$, have been outlined with solid lines while the rest of each beam is defined by dashed lines. For each beam the origin of the coordinate ξ is seen to lie at a different position relative to the end where a unit positive moment is suddenly applied at time $\tau = 0$. An infinite number of these beams is assumed to exist.

The response of the top beam has already been determined as (eqs. (C25) and (C26))

$$Z(\xi, \tau) = 2\lambda_1 e^{i\lambda_1 \tau} J_0(\lambda \sqrt{\tau^2 - \xi^2}) \quad (\tau > \xi)$$

and

$$K(\xi, \tau) = G(\xi, \tau) \quad (\tau > \xi)$$

where

$$G(\xi, \tau) = e^{i\lambda\xi} - \lambda\xi \int_{\xi}^{\tau} e^{i\lambda\theta} \frac{J_1(\lambda\sqrt{\theta^2 - \xi^2})}{\sqrt{\theta^2 - \xi^2}} d\theta$$

The response of the second beam may be determined from these equations simply by accounting for the changed direction and shifted origin of the coordinate ξ . This process gives

$$Z(\xi, \tau) = 2\lambda i e^{i\lambda\tau} J_0 \left[\lambda \sqrt{\tau^2 - (2 - \xi)^2} \right] \quad (\tau > 2 - \xi)$$

and

$$K(\xi, \tau) = -G(2 - \xi, \tau) \quad (\tau > 2 - \xi)$$

In order to obtain the response of the third beam from the response of the first, only the shifted origin need be accounted for. Thus, for this beam,

$$Z(\xi, \tau) = 2\lambda i e^{i\lambda\tau} J_0 \left[\lambda \sqrt{\tau^2 - (2 + \xi)^2} \right] \quad (\tau > 2 + \xi)$$

$$K(\xi, \tau) = G(2 + \xi, \tau) \quad (\tau > 2 + \xi)$$

Similarly, for the fourth beam,

$$Z(\xi, \tau) = 2\lambda i e^{i\lambda\tau} J_0 \left[\lambda \sqrt{\tau^2 - (4 - \xi)^2} \right] \quad (\tau > 4 - \xi)$$

$$K(\xi, \tau) = -G(4 - \xi, \tau) \quad (\tau > 4 - \xi)$$

and so forth, for all the rest. In each case, the region where the response is not specified is a region of zero response.

Let the responses of all these beams to their respective disturbances be superposed and consider only the response of the segment $0 \leq \xi \leq 1$ of the resulting composite beam. Since the wave fronts of all the disturbances travel at the same velocity $\frac{d\xi}{d\tau} = 1$, the response of this segment may be written

$$\left. \begin{aligned}
 Z(\xi, \tau) &= 0 & (0 \leq \tau \leq \xi) \\
 Z(\xi, \tau) &= 2\lambda i e^{i\lambda\tau} J_0(\lambda\sqrt{\tau^2 - \xi^2}) & (\xi \leq \tau \leq 2 - \xi) \\
 Z(\xi, \tau) &= 2\lambda i e^{i\lambda\tau} \left\{ J_0(\lambda\sqrt{\tau^2 - \xi^2}) + \right. \\
 &\quad \left. J_0[\lambda\sqrt{\tau^2 - (2 - \xi)^2}] \right\} & (2 - \xi \leq \tau \leq 2 + \xi) \\
 Z(\xi, \tau) &= 2\lambda i e^{i\lambda\tau} \left\{ J_0(\lambda\sqrt{\tau^2 - \xi^2}) + J_0[\lambda\sqrt{\tau^2 - (2 - \xi)^2}] + \right. \\
 &\quad \left. J_0[\lambda\sqrt{\tau^2 - (2 + \xi)^2}] \right\} & (2 + \xi \leq \tau \leq 4 - \xi)
 \end{aligned} \right\} \quad (C33)$$

and

$$\left. \begin{aligned}
 K(\xi, \tau) &= 0 & (0 \leq \tau \leq \xi) \\
 K(\xi, \tau) &= G(\xi, \tau) & (\xi \leq \tau \leq 2 - \xi) \\
 K(\xi, \tau) &= G(\xi, \tau) - G(2 - \xi, \tau) & (2 - \xi \leq \tau \leq 2 + \xi) \\
 K(\xi, \tau) &= G(\xi, \tau) - G(2 - \xi, \tau) + G(2 + \xi, \tau) & (2 + \xi \leq \tau \leq 4 - \xi)
 \end{aligned} \right\} \quad (C34)$$

Since $G(0, \tau) = 1$, equations (C34) are seen to satisfy the boundary conditions (C32) and the response obtained above must be that of a simply supported uniform beam to a unit dimensionless step moment applied at the support $\xi = 0$.

The vertical shear \bar{V} and bending moment \bar{M} may be obtained from equations (C33) and (C34) as

$$\left. \begin{aligned}
 \bar{V}(\xi, \tau) &= 0 & (0 \leq \tau \leq \xi) \\
 \bar{V}(\xi, \tau) &= -2\lambda \sin \lambda \tau J_0(\lambda \sqrt{\tau^2 - \xi^2}) & (\xi \leq \tau \leq 2 - \xi) \\
 \bar{V}(\xi, \tau) &= -2\lambda \sin \lambda \tau \left\{ J_0(\lambda \sqrt{\tau^2 - \xi^2}) + \right. \\
 &\quad \left. J_0[\lambda \sqrt{\tau^2 - (2 - \xi)^2}] \right\} & (2 - \xi \leq \tau \leq 2 + \xi) \\
 \bar{V}(\xi, \tau) &= -2\lambda \sin \lambda \tau \left\{ J_0(\lambda \sqrt{\tau^2 - \xi^2}) + J_0[\lambda \sqrt{\tau^2 - (2 - \xi)^2}] + \right. \\
 &\quad \left. J_0[\lambda \sqrt{\tau^2 - (2 + \xi)^2}] \right\} & (2 + \xi \leq \tau \leq 4 - \xi)
 \end{aligned} \right\} \quad (C35)$$

and

$$\left. \begin{aligned}
 \bar{M}(\xi, \tau) &= 0 & (0 \leq \tau \leq \xi) \\
 \bar{M}(\xi, \tau) &= H(\xi, \tau) & (\xi \leq \tau \leq 2 - \xi) \\
 \bar{M}(\xi, \tau) &= H(\xi, \tau) - H(2 - \xi, \tau) & (2 - \xi \leq \tau \leq 2 + \xi) \\
 \bar{M}(\xi, \tau) &= H(\xi, \tau) - H(2 - \xi, \tau) + H(2 + \xi, \tau) & (2 + \xi \leq \tau \leq 4 - \xi)
 \end{aligned} \right\} \quad (C36)$$

where

$$H(\xi, \tau) = \cos \lambda \xi - \lambda \xi \int_{\xi}^{\tau} \cos \lambda \theta \frac{J_1(\lambda \sqrt{\theta^2 - \xi^2})}{\sqrt{\theta^2 - \xi^2}} d\theta$$

The angular and linear velocities $\bar{\omega}$ and \bar{v} may, of course, also be obtained from equations (C33) and (C34).

Computations have been made for the quantity $\bar{V}(0, \tau)$ from equation (C35) with $\lambda = 5$. The results have been plotted in figure 5(a) in the range $0 \leq \tau \leq 8$.

Finite simply supported beam with an applied ramp-platform end moment.— Let the applied moment at the end $\xi = 0$ of a simply supported uniform beam have the time history

$$\left. \begin{aligned} \bar{M}(0, \tau) &= \tau & (0 \leq \tau \leq 1) \\ \bar{M}(0, \tau) &= 1 & (\tau > 1) \end{aligned} \right\} \quad (C37)$$

The response of the beam to this disturbance may be obtained from the response to a unit step by using Duhamel's superposition integral. Thus, if the response to a unit step, as given by equation (C33), is designated $Z_1(\xi, \tau)$, the response $Z(\xi, \tau)$ to the applied moment (C37) may be written

$$\left. \begin{aligned} Z(\xi, \tau) &= \int_0^{\tau} Z_1(\xi, \tau - \theta) d\theta & (0 \leq \tau \leq 1) \\ Z(\xi, \tau) &= \int_0^1 Z_1(\xi, \tau - \theta) d\theta & (\tau > 1) \end{aligned} \right\} \quad (C38)$$

Substituting from equations (C33) and letting $\xi = 0$ results in the following expressions for the end response $Z(0, \tau)$:

$$\begin{aligned}
 Z(0, \tau) &= 2\lambda i \int_0^\tau e^{i\lambda(\tau-\theta)} J_0[\lambda(\tau - \theta)] d\theta & (0 \leq \tau \leq 1) \\
 Z(0, \tau) &= 2\lambda i \int_0^1 e^{i\lambda(\tau-\theta)} J_0[\lambda(\tau - \theta)] d\theta & (1 \leq \tau \leq 2) \\
 Z(0, \tau) &= 2\lambda i \int_0^1 e^{i\lambda(\tau-\theta)} J_0[\lambda(\tau - \theta)] d\theta + \\
 &\quad 4\lambda i \int_0^{\tau-2} e^{i\lambda(\tau-\theta)} J_0[\lambda\sqrt{(\tau - \theta)^2 - 4}] d\theta & (2 \leq \tau \leq 3) \\
 Z(0, \tau) &= 2\lambda i \int_0^1 e^{i\lambda(\tau-\theta)} J_0[\lambda(\tau - \theta)] d\theta + \\
 &\quad 4\lambda i \int_0^1 e^{i\lambda(\tau-\theta)} J_0[\lambda\sqrt{(\tau - \theta)^2 - 4}] d\theta & (3 \leq \tau \leq 4) \\
 Z(0, \tau) &= 2\lambda i \int_0^1 e^{i\lambda(\tau-\theta)} J_0[\lambda(\tau - \theta)] d\theta + \\
 &\quad 4\lambda i \int_0^1 e^{i\lambda(\tau-\theta)} J_0[\lambda\sqrt{(\tau - \theta)^2 - 4}] d\theta + \\
 &\quad 4\lambda i \int_0^{\tau-4} e^{i\lambda(\tau-\theta)} J_0[\lambda\sqrt{(\tau - \theta)^2 - 16}] d\theta & (4 \leq \tau \leq 5)
 \end{aligned}
 \tag{C39}$$

It can be seen that (transforms 3, 4, and 9, table I)

$$L \left\{ \int_0^\tau e^{i\lambda\theta} J_0(\lambda\theta) d\theta \right\} = \frac{1}{p\sqrt{p(p-2\lambda i)}} = -\frac{1}{\lambda} \frac{d}{dp} \left(\sqrt{\frac{p-2\lambda i}{p}} - 1 \right)$$

or (transforms 5 and 11, table I)

$$\int_0^\tau e^{i\lambda\theta} J_0(\lambda\theta) d\theta = \tau e^{i\lambda\tau} [\bar{J}_0(\lambda\tau) - iJ_1(\lambda\tau)]$$

Then, $Z(0, \tau)$ may be reduced in the region $0 \leq \tau \leq 2$ to

$$Z(0, \tau) = 2\lambda i \int_0^\tau e^{i\lambda\theta} J_0(\lambda\theta) d\theta$$

$$Z(0, \tau) = 2\lambda i \tau e^{i\lambda\tau} [\bar{J}_0(\lambda\tau) - iJ_1(\lambda\tau)] \quad (0 \leq \tau \leq 1) \quad (C40)$$

and

$$\begin{aligned} Z(0, \tau) &= 2\lambda i \int_{\tau-1}^\tau e^{i\lambda\theta} J_0(\lambda\theta) d\theta \\ &= 2\lambda i \left[\int_0^\tau e^{i\lambda\theta} J_0(\lambda\theta) d\theta - \int_0^{\tau-1} e^{i\lambda\theta} J_0(\lambda\theta) d\theta \right] \end{aligned}$$

$$Z(0, \tau) = 2\lambda i \tau e^{i\lambda\tau} [\bar{J}_0(\lambda\tau) - iJ_1(\lambda\tau)] -$$

$$2\lambda i(\tau-1)e^{i\lambda(\tau-1)} \left\{ \bar{J}_0[\lambda(\tau-1)] - iJ_1[\lambda(\tau-1)] \right\}$$

$$(1 \leq \tau \leq 2) \quad (C41)$$

From these equations, the shear at $\xi = 0$ may be written in this range as

$$\left. \begin{aligned} \bar{V}(0, \tau) &= 2\lambda\tau [\cos \lambda\tau J_1(\lambda\tau) - \sin \lambda\tau J_0(\lambda\tau)] & (0 \leq \tau \leq 1) \\ \bar{V}(0, \tau) &= 2\lambda\tau [\cos \lambda\tau J_1(\lambda\tau) - \sin \lambda\tau J_0(\lambda\tau)] - \\ &\quad 2\lambda(\tau - 1) \left\{ \cos \lambda(\tau - 1) J_1[\lambda(\tau - 1)] - \right. \\ &\quad \left. \sin \lambda(\tau - 1) J_0[\lambda(\tau - 1)] \right\} & (1 \leq \tau \leq 2) \end{aligned} \right\} \quad (C42)$$

In the range $\tau > 2$, however, the integrals in equations (C39) apparently cannot be evaluated analytically. If the shear $\bar{V}_1(0, \tau)$ due to a unit step moment has been computed, it may be convenient to write, for the shear at the point $\xi = 0$ resulting from the disturbance (C37),

$$\left. \begin{aligned} \bar{V}(0, \tau) &= \int_0^\tau \bar{V}_1(0, \tau - \theta) d\theta & (0 \leq \tau \leq 1) \\ \bar{V}(0, \tau) &= \int_0^1 \bar{V}_1(0, \tau - \theta) d\theta & (\tau > 1) \end{aligned} \right\} \quad (C43)$$

and then evaluate the integral $\int_0^1 \bar{V}_1(0, \tau - \theta) d\theta$ numerically to obtain $\bar{V}(0, \tau)$ in the range $\tau > 2$.

The quantity $\bar{V}(0, \tau)$, for a beam with $\lambda = 5$, has been computed in the range $0 \leq \tau \leq 2$ from equations (C42) and has been obtained in the range $2 \leq \tau \leq 8$ by a numerical integration of the exact curve of figure 5(a) in accordance with equation (C43). These results are presented in figure 6(a).

REFERENCES

1. Biot, M. A., and Bisplinghoff, R. L.: Dynamic Loads on Airplane Structures During Landing. NACA WR W-92, 1944. (Formerly NACA ARR 4H10.)
2. Williams, D.: Displacements of a Linear Elastic System Under a Given Transient Load. British S.M.E. C/7219/DW/19, Aug. 1946.
3. Isakson, G.: A Survey of Analytical Methods for Determining Transient Stresses in Elastic Structures. Contract No. N5 ori-07833, Office Naval Res. (Project NR-035-259), M.I.T., Mar. 3, 1950.
4. Ramberg, Walter: Transient Vibration in an Airplane Wing Obtained by Several Methods. Res. Paper RP1984, Nat. Bur. of Standards Jour. Res., vol. 42, no. 5, May 1949, pp. 437-447.
5. Kruszewski, Edwin T.: Effect of Transverse Shear and Rotary Inertia on the Natural Frequency of a Uniform Beam. NACA TN 1909, 1949.
6. Flügge, W.: Die Ausbreitung von Biegungswellen in Stäben. Z.a.M.M., Bd. 22, Nr. 6, Dec. 1942, pp. 312-318.
7. Timoshenko, S.: Vibration Problems in Engineering. Second ed., D. Van Nostrand Co., Inc., 1937, pp. 337-338.
8. Robinson, A.: Shock Transmission in Beams. R. & M. No. 2265, British A.R.C., 1945.
9. Pfeiffer, F.: Über die Differentialgleichung der transversalen Stabschwingungen. Z.a.M.M., Bd. 25/27, Nr. 3, June 1947, pp. 83-91.
10. Uflyand, Y. S.: Propagation of Waves in Transverse Vibrations of Beams and Plates. Prikladnaya Matematika i Mekhanika (U. S. S. R.), vol. XII, no. 3, May-June 1948, pp. 287-300.
11. Dengler, M. A., and Goland, M.: Transverse Impact of Long Beams, Including Rotatory-Inertia and Shear Effects. Midwest Res. Inst. (Kansas City, Mo.). (To be published in the Proceedings of the First U. S. Nat. Congress of Appl. Mech. (Chicago), June 11-16, 1951.)
12. Courant, R., and Friedrichs, K. O.: Supersonic Flow and Shock Waves. Pure & Appl. Math., vol. I, Interscience Publishers, Inc. (New York), 1948, pp. 38-59.

13. Prescott, John: Elastic Waves and Vibrations of Thin Rods. Phil. Mag., ser. 7, vol. 33, no. 225, Oct. 1942, pp. 703-754.
14. Cooper, J. L. B.: The Propagation of Elastic Waves in a Rod. Phil. Mag., ser. 7, vol. 38, no. 276, Jan. 1947, pp. 1-22.
15. Churchill, Ruel V.: Modern Operational Mathematics in Engineering. McGraw-Hill Book Co., Inc., 1944.
16. Campbell, George A., and Foster, Ronald M.: Fourier Integrals for Practical Applications. Monograph B-584, Bell Telephone System, 1942.
17. McLachlan, N. W.: Bessel Functions for Engineers. Clarendon Press (Oxford), 1934.
18. Jahnke, Eugene, and Emde, Fritz: Tables of Functions. Fourth ed., Dover Publications, 1945, p. 144.

TABLE I.- LAPLACE TRANSFORMS

Number	$F(\tau)$ (a)		$f(p) = \int_0^\infty e^{-p\tau} F(\tau) d\tau$	Reference
1	$\int_0^\tau F_1(\tau - \theta) F_2(\theta) d\theta$ $(\tau > 0)$		$f_1(p) f_2(p)$	15
2	$F(\tau - \xi)$ $(\tau > \xi)$		$e^{-\xi p} f(p)$	15
3	$e^{i\lambda\tau} F(\tau)$ $(\tau > 0)$		$f(p - i\lambda)$	15
4	$\int_0^\tau F(\theta) d\theta$ $(\tau > 0)$		$\frac{1}{p} f(p)$	15
5	$\tau F(\tau)$ $(\tau > 0)$		$-f'(p)$	15
6	$F^n(\tau) = \frac{d^n}{d\tau^n} [F(\tau)]$ $(\tau > 0)$		$p^n f(p) - p^{n-1} F(+0) - p^{n-2} F'(+0) - \dots - p^{n-1} F^{(n-1)}(+0)$	15
7	1 $(\tau > 0)$		$\frac{1}{p}$	15
8	τ $(\tau > 0)$		$\frac{1}{p^2}$	15
9	$J_0(\lambda\tau)$ $(\tau > 0)$		$\frac{1}{\sqrt{p^2 + \lambda^2}}$	15
10	$J_1(\lambda\tau)$ $(\tau > 0)$		$\frac{1}{\lambda} \left(1 - \frac{p}{\sqrt{p^2 + \lambda^2}} \right)$	15
11	$e^{i\lambda\tau} [J_0(\lambda\tau) - iJ_1(\lambda\tau)]$ $(\tau > 0)$		$\frac{1}{\lambda} \left(\sqrt{\frac{p - i2\lambda}{p}} - 1 \right)$	--
12	$e^{-i\lambda\tau} [J_0(\lambda\tau) + iJ_1(\lambda\tau)]$ $(\tau > 0)$		$\frac{1}{\lambda} \left(1 - \sqrt{\frac{p + i2\lambda}{p}} \right)$	--
13	$\cos \lambda\tau J_0(\lambda\tau) + \sin \lambda\tau J_1(\lambda\tau)$ $(\tau > 0)$		$\frac{1}{2\lambda} \left(\sqrt{\frac{p - i2\lambda}{p}} - \sqrt{\frac{p + i2\lambda}{p}} \right)$	--
14	$\frac{2\lambda}{\tau} J_1(2\lambda\tau)$ $(\tau > 0)$		$\sqrt{p^2 + 4\lambda^2} - p$	15
15	$J_0(\lambda\sqrt{\tau^2 - \xi^2})$ $(\tau > \xi)$		$\frac{e^{-\xi\sqrt{p^2 + \lambda^2}}}{\sqrt{p^2 + \lambda^2}}$	15
16	$\frac{\lambda \xi J_1(\lambda\sqrt{\tau^2 - \xi^2})}{\sqrt{\tau^2 - \xi^2}}$ $(\tau > \xi)$		$e^{-\xi p} - e^{-\xi\sqrt{p^2 + \lambda^2}}$	15
17	$\frac{\tau J_1(\lambda\sqrt{\tau^2 - \xi^2})}{\sqrt{\tau^2 - \xi^2}} + iJ_0(\lambda\sqrt{\tau^2 - \xi^2})$ $(\tau > \xi)$		$\frac{1}{\lambda} \left(e^{-\xi p} - \sqrt{\frac{p - i\lambda}{p + i\lambda}} e^{-\xi\sqrt{p^2 + \lambda^2}} \right)$	16

^a $F(\tau) = 0$ for all values of τ not specified.

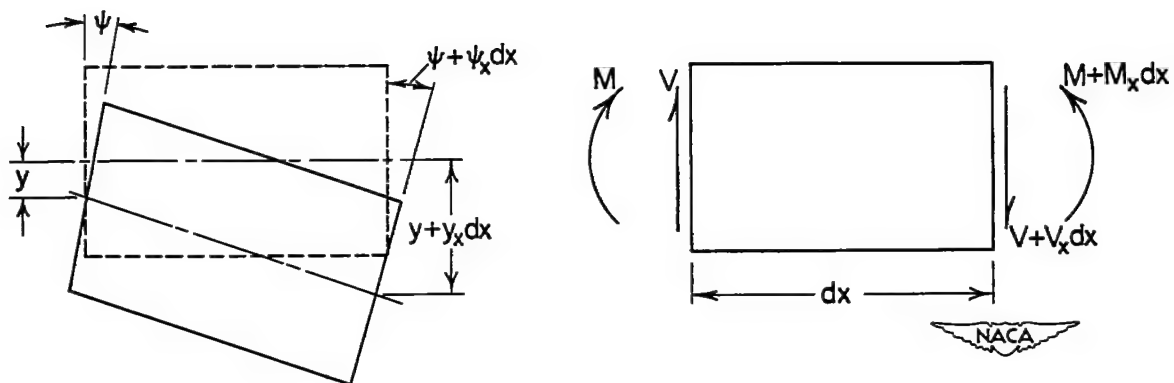


Figure 1.- Positive distortions and positive internal forces and moments associated with a typical beam element.

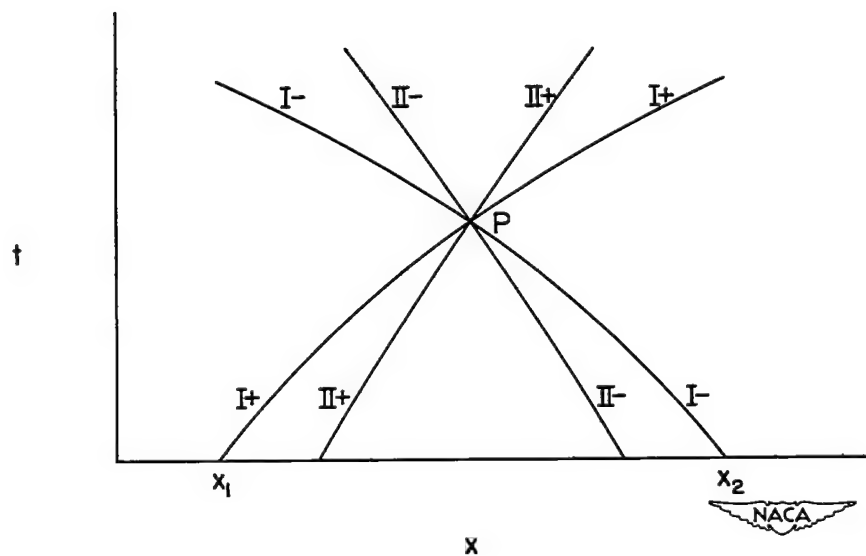
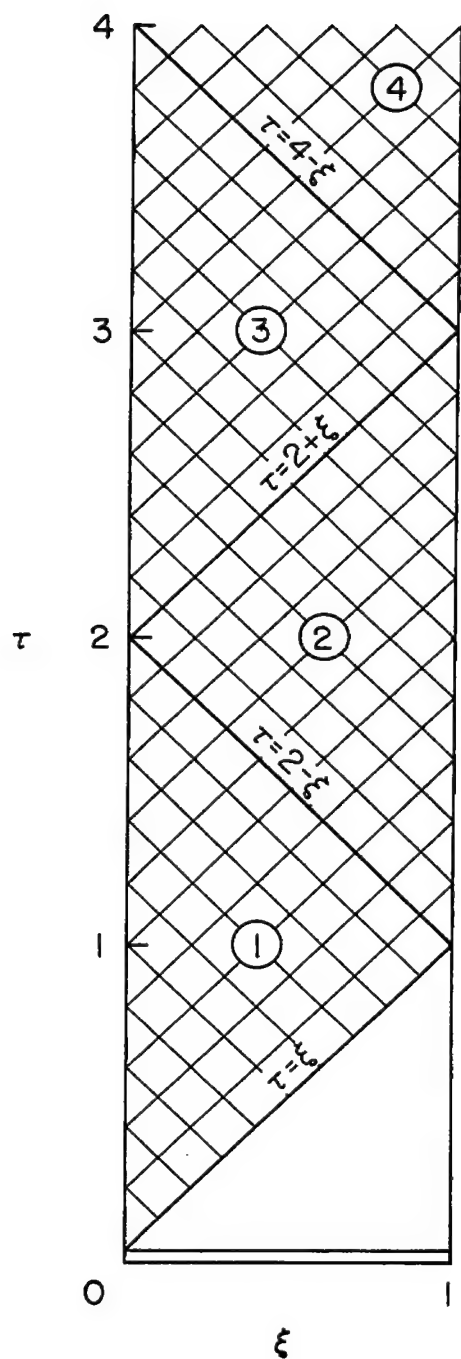
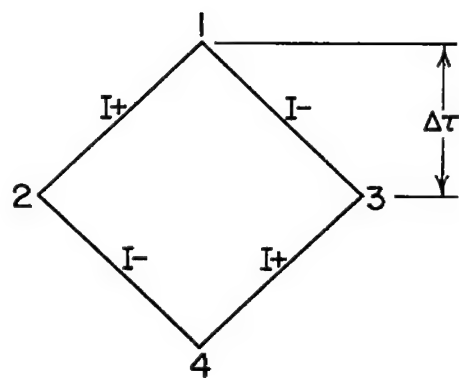


Figure 2.- The characteristics of Timoshenko's equations for a point in the x, t plane.



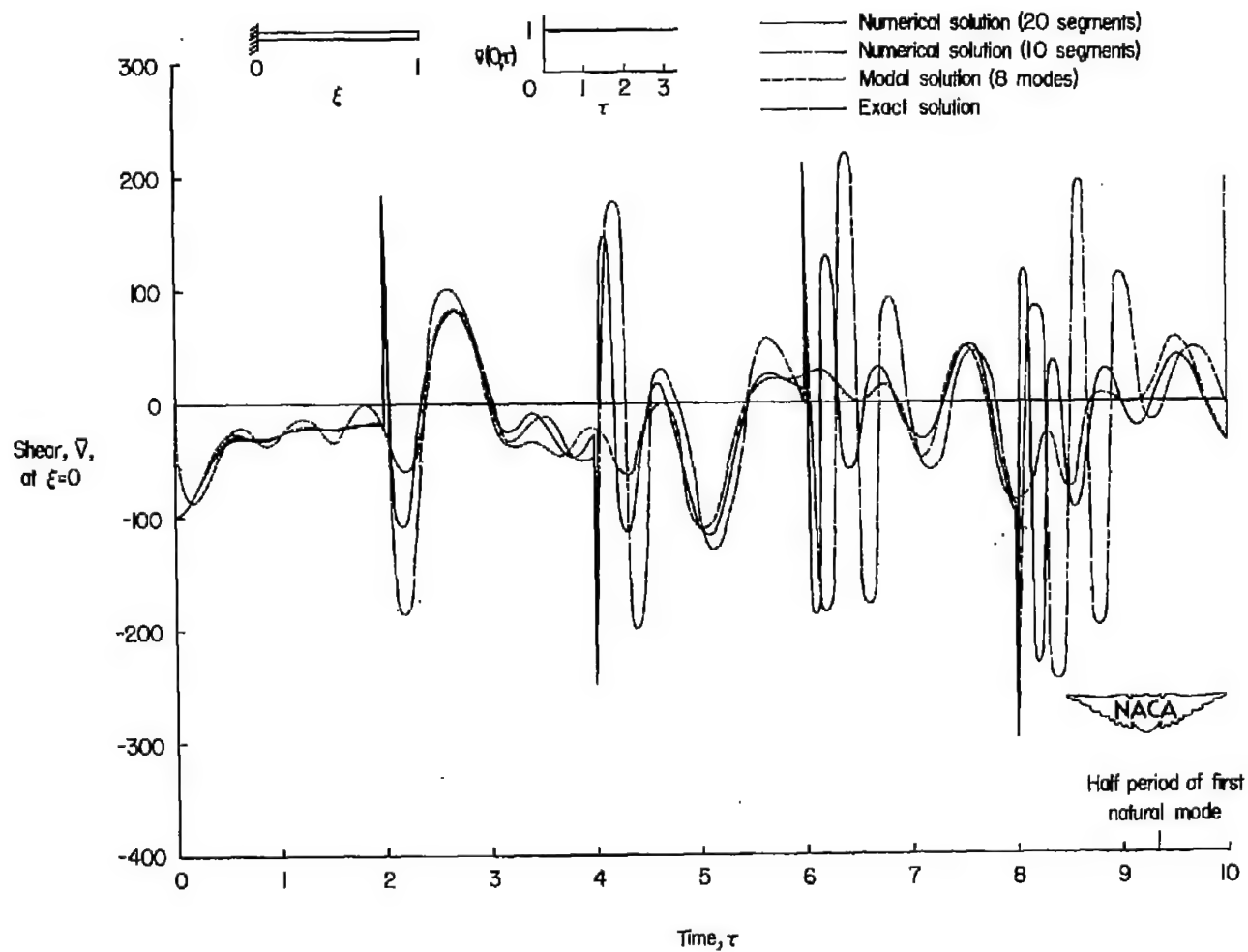
(a) Space-time plane.



(b) Typical interior mesh.

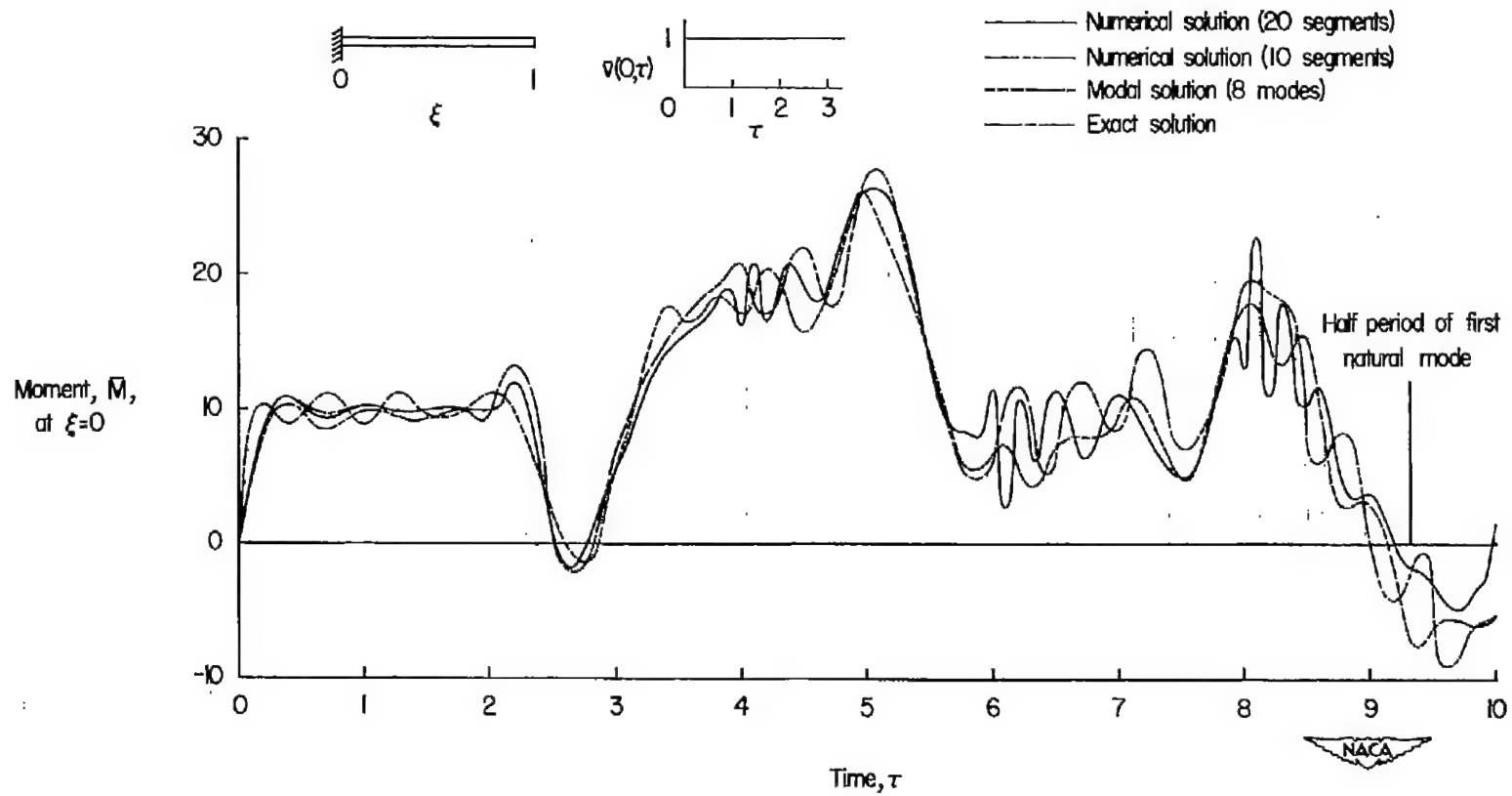


Figure 3.- Characteristic grid for application of numerical procedure to uniform beams with disturbance applied at $\xi = 0$. $c_1 = c_2$.



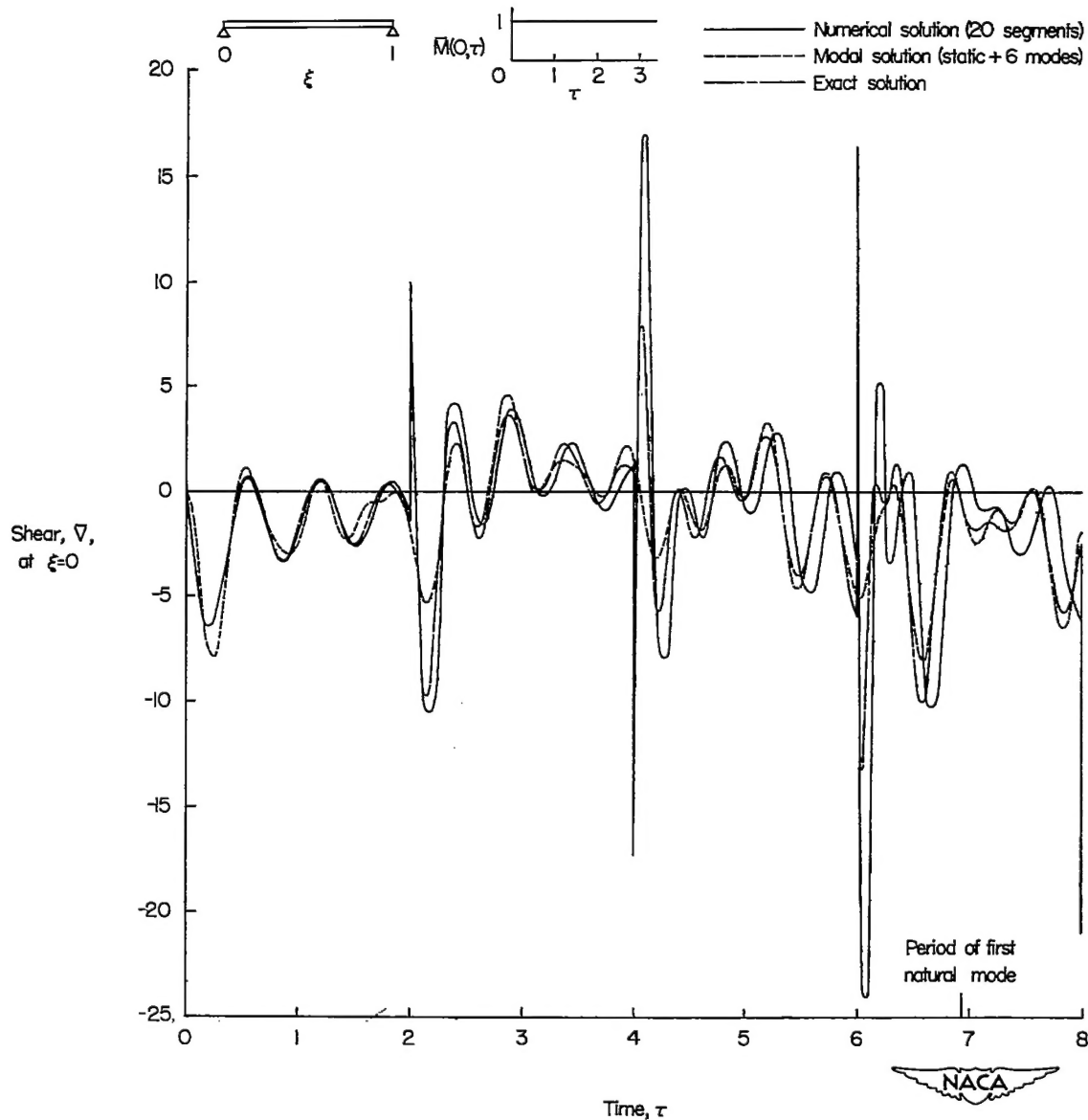
(a) Time history of the nondimensional vertical shear at the root.

Figure 4.- Response of a uniform cantilever beam subjected to a step velocity at the root.



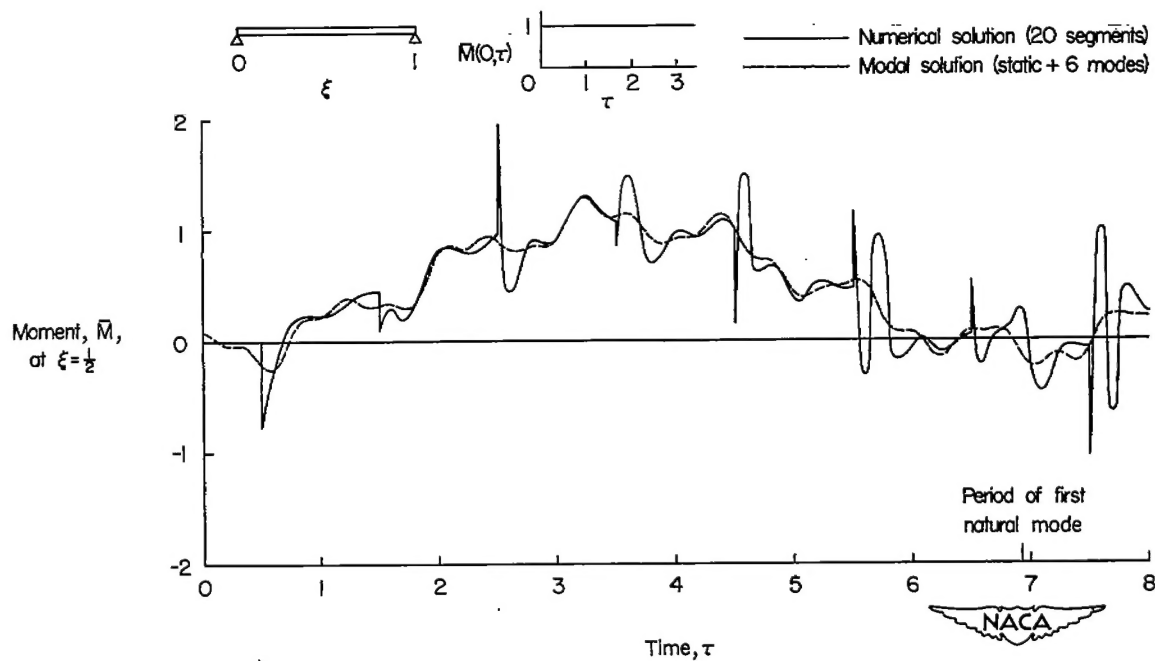
(b) Time history of the nondimensional moment at the root.

Figure 4.- Concluded.



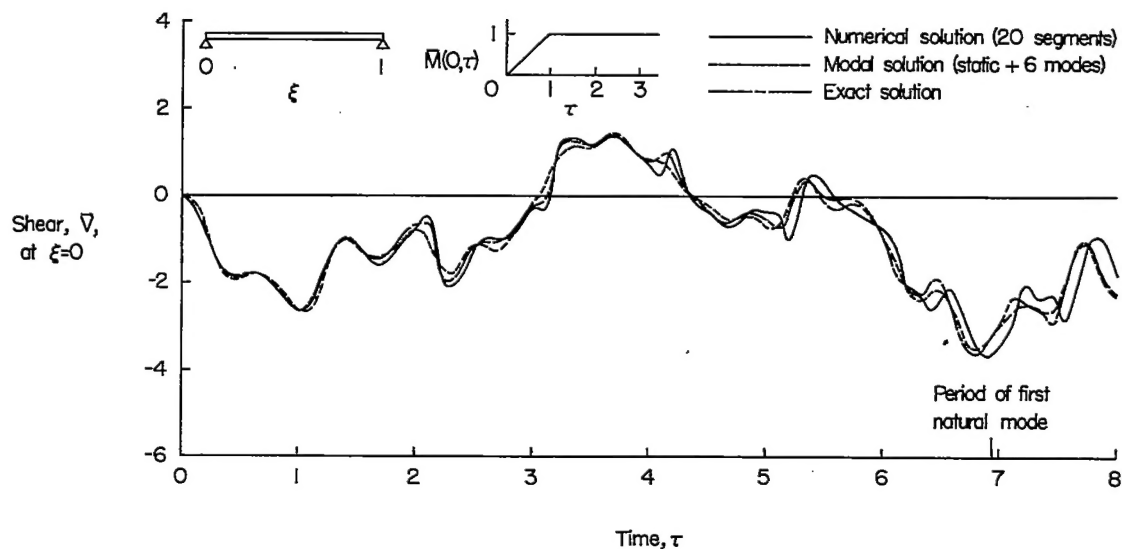
(a) Time history of the nondimensional vertical shear at the end $\xi = 0$.

Figure 5.- Response of a uniform simply supported beam subjected to a step moment at $\xi = 0$.

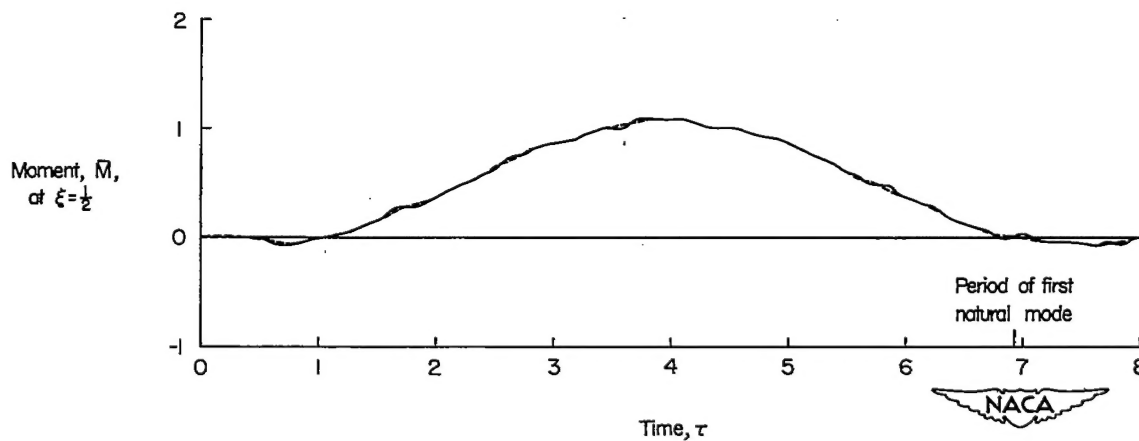


(b) Time history of the nondimensional moment at the center.

Figure 5.- Concluded.



(a) Time history of the nondimensional vertical shear at the end $\xi = 0$.



(b) Time history of the nondimensional moment at the center.

Figure 6.- Response of a uniform simply supported beam subjected to a ramp-platform moment at $\xi = 0$.

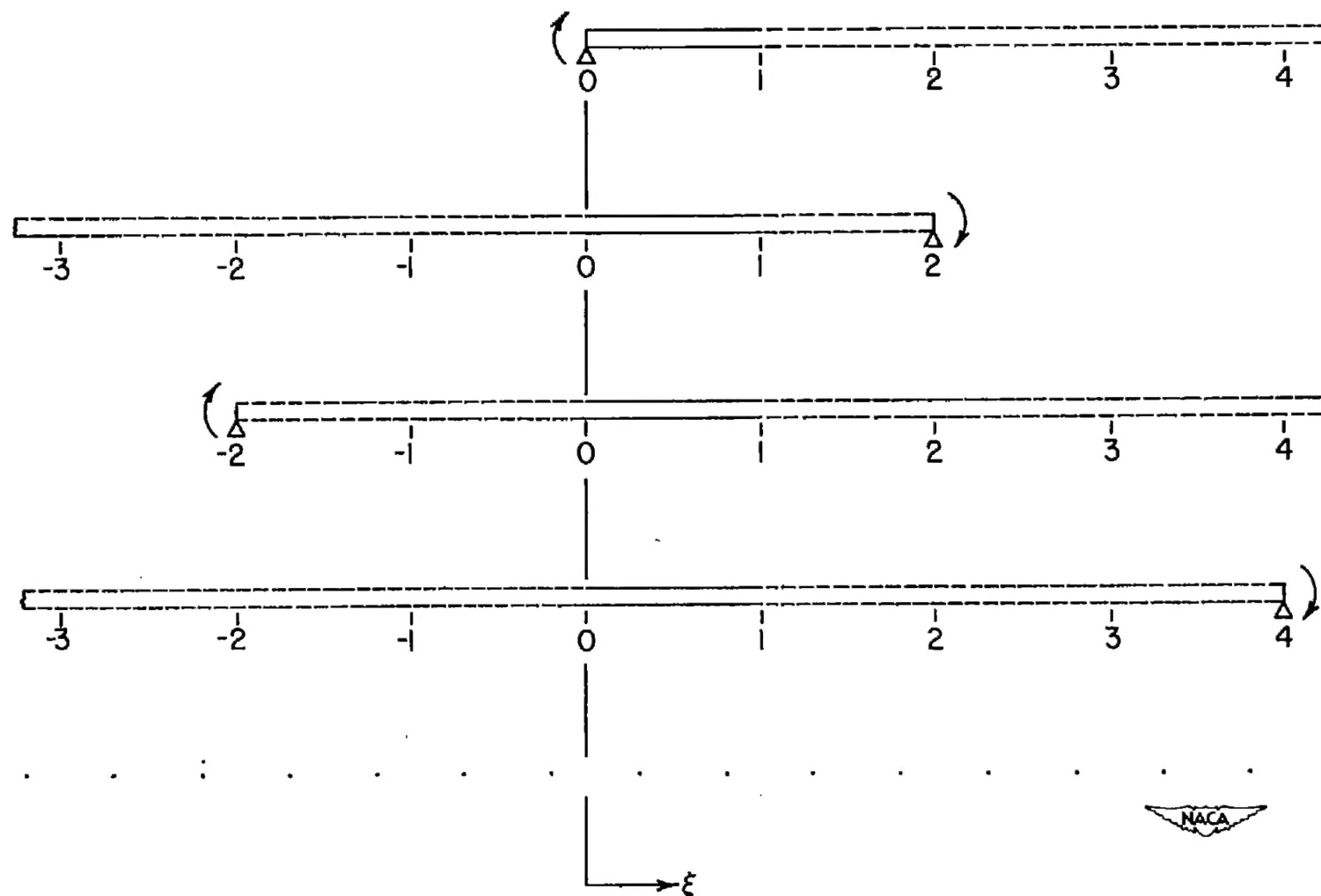


Figure 7.- Semi-infinite uniform beams superposed to obtain the response of a finite simply supported beam.